Distribution Agreement

In presenting this thesis or dissertation as a partial fulfillment of the requirements for an advanced degree from Emory University, I hereby grant to Emory University and its agents the non-exclusive license to archive, make accessible, and display my thesis or dissertation in whole or in part in all forms of media, now or hereafter known, including display on the world wide web. I understand that I may select some access restrictions as part of the online submission of this thesis or dissertation. I retain all ownership rights to the copyright of the thesis or dissertation. I also retain the right to use in future works (such as articles or books) all or part of this thesis or dissertation.

Signature:

_____ _____

Haley Lei Huang Date

Induction of anti-tumor immunity by vaccine immunotherapy in murine lung cancer models

By

Haley Lei Huang

Mater of Science

Graduate Division of Biological and Biomedical Sciences

Cancer Biology and Translational Oncology

_____

Periasamy Selvaraj, Ph.D.
Advisor

_____

Ramireddy Bommireddy, Ph.D.
Advisor

_____

Mellissa Gilbert-Ross, Ph.D.
Committee Member

_____

Rita Nahta, Ph.D.
Committee Member

Accepted:

_____

Lisa A. Tedesco, Ph.D.
Dean of the James T. Laney School of Graduate Studies

_____

Date

Induction of anti-tumor immunity by vaccine immunotherapy in murine lung cancer models

By

Haley Lei Huang
B.S. Emory University, 2018

Advisor: Periasamy Selvaraj, Ph.D

An abstract of
A thesis submitted to the Faculty of the
James T. Laney School of Graduate Studies of Emory University
in partial fulfillment of the requirements for the degree of
Master of Science in Cancer Biology and Translational Oncology
in the Graduate Division of Biological and Biomedical sciences
2019

Abstract

Induction of anti-tumor immunity by vaccine immunotherapy in murine lung cancer models

By Haley Lei Huang

Lung cancer is the leading cause of cancer deaths in the world. Despite the development of novel treatments in the recent years such as immune checkpoint inhibitor (ICI) therapy, the prognosis of lung cancer patients is still poor. The patient-to-patient heterogeneity is the major problem in treating lung cancer, which results in differential responses to ICI therapy. In this study, two projects were designed to induce the anti-tumor immunity by using vaccine immunotherapy or foreign protein transfection to introduce novel antigen presentation in ICI resistant murine lung cancer models. In the first project, we developed a vaccine immunotherapy prepared by tumor membrane vesicle (TMV), which express tumor-specific antigens, further modified to express immunostimulatory molecules (ISMs). We investigated the efficacy of the ISM-incorporated TMV vaccine (TMVV) in combination with ICI therapy in a partially ICI resistant murine lung cancer model. We demonstrate that prophylactic vaccination of TMV adjuvanted with IL-12 and B7-1 prevents the CMT-167 tumor growth and helps the mice develop immunological memory. In a therapeutic setting, TMVV immunotherapy induced primary tumor regression in 40% of the mice and significantly reduced the metastatic tumor burden. Moreover, stimulation of splenocytes with TMVV induces IFN- γ secretion, which can upregulate the level of MHC I and MHC II on CMT-167 cells. We also find that prophylactic TMVV immunotherapy stimulates MHC II-dependent CD4+ T cells-mediated cytotoxic activity, while CD8+ T lymphocytes are indispensable for a complete effect of the vaccination. In the second project, we transfected a fully ICI resistant murine lung cancer model with a foreign antigen, red fluorescent protein (RFP) and investigated its response to the vaccine immunotherapy. Our findings suggest that the expression of RFP in LL/2 cells induces tumor immunogenicity by increasing TILs and inhibiting tumor-induced G-CSF and MDSC levels. In addition, prophylactic TMV immunotherapy primes the immune system and boosts the anti-tumor immune response in LL/2-RFP-tumor bearing mice by further inducing TILs and inhibiting immunosuppressive G-CSF and MDSC levels. Overall, our studies provide insight into using immunotherapy to regulate novel antigen presentation for treating ICI resistant lung cancer.

Induction of anti-tumor immunity by vaccine immunotherapy in murine lung cancer models

By

Haley Lei Huang
B.S. Emory University, 2018

Advisor: Periasamy Selvaraj, Ph.D

A thesis submitted to the Faculty of the
James T. Laney School of Graduate Studies of Emory University
in partial fulfillment of the requirements for the degree of
Master of Science in Cancer Biology and Translational Oncology
in the Graduate Division of Biological and Biomedical sciences
2019

Table of Contents

Project I - Immunotherapy with TMV vaccine induces CD4+ T cell mediated antitumor immunity in a partially ICI resistant murine lung cancer model

Table of Figures

Project I

Project II

PROJECT I

Immunotherapy with TMV vaccine induces CD4+ T cell mediated antitumor immunity in a partially ICI resistant murine lung cancer model

INTRODUCTION

Lung cancer has been the leading cause of cancer deaths in both men and women worldwide since 1985[1]. In 2019, there will be approximately 228,150 people diagnosed with lung cancer and 142,670 deaths in the United States[2]. Lung cancer can be classified into two types: non-small cell lung cancer (NSCLC), which accounts for 85% of cases and small cell lung cancer (SCLC), which accounts for the remaining 15% of cases[1]. The main difficulties in lung cancer treatment are the lack of early diagnostic tools and patient to patient heterogeneity of cancer [3]. The major treatment options for lung cancer patients are surgery for early-stage disease, radiotherapy and chemotherapy for advanced-stage disease, but the survival rate for lung cancer patients remains low[4]. The discovery of immune checkpoint inhibitor (ICI) therapy has made a breakthrough in the treatment for lung cancer[5]. However, only a subset of patients responds well to ICI therapy, while other patients are resistant to immune checkpoint blockade[5]. Therefore, to overcome the challenge of global lung cancer mortality, a number of studies are being conducted to improve lung cancer prevention and treatment.

In the current study, we developed a vaccine immunotherapy prepared from tumor tissue. Specifically, tumor tissue was homogenized to get tumor membrane vesicles (TMVs) and further modified with glycosylphosphatidylinositol (GPI)-anchored immunostimulatory molecules (ISMs) IL-12 and B7-1. The rationale of using these two membrane-anchored ISMs is that previous research has shown membrane-anchored ISMs effectively induce anti-tumor immune response locally at the vaccination site, which is potentially less toxic to patients compared to systemic administration of cytokines[6, 7]. Moreover, it has been shown that B7-1 (CD80) provides essential co-stimulation needed for T cell activation[8], while IL-12 activates dendritic cells (DCs), induces a Th1 response and stimulates IFN-γ secretion from T cells and natural killer (NK) cells[9]. Therefore,

the ISM-incorporated TMV vaccine (TMVV) not only present distinct tumor antigens originally expressed on different clonal populations of tumor tissue samples, but also present GPI-IL-12 and GPI-B7-1 to stimulate immune response at the vaccination site.

To investigate the efficacy of the ISM-incorporated TMV vaccine, we conducted both prophylactic and therapeutic vaccination study using CMT-167 tumor model. CMT-167 tumor cell model was established from alveolar lung carcinoma of C57BL/6 female mice by LM. Franks, et al. in 1976[10]. In the prophylactic setting, we investigated whether vaccination of TMV adjuvanted with IL-12 and B7-1 prevents the CMT-167 tumor growth in mice and helps the mice develop immunological memory to the tumor cell challenge. Moreover, our preliminary data have shown that primary tumor growth of CMT-167 cells were partially inhibited by anti-PD-1 antibody therapy (Fig. 1). Hence, in the therapeutic setting, we studied whether the combination of TMV vaccine with anti-PD-1 mAb could induce more complete primary tumor regression and/ or reduce metastatic tumor burden. Furthermore, to study the possible mechanism of immune activation in response to TMV vaccine, an *in vivo* cellular depletion study and *in vitro* cytotoxic T lymphocyte assay were conducted to assess the role of CD4+ T cells, CD8+ T cells, and NK cells in TMVV-mediated anti-tumor immunity. Finally, cellular phenotyping of immune infiltrates was performed by using Matrigel to pinpoint the specific cellular interactions in the immune response induced by TMV vaccine. Overall, our studies provide insight into using the immunotherapy of TMV adjuvanted with membrane-anchored ISMs for treating the partially ICI resistant lung cancer patients.

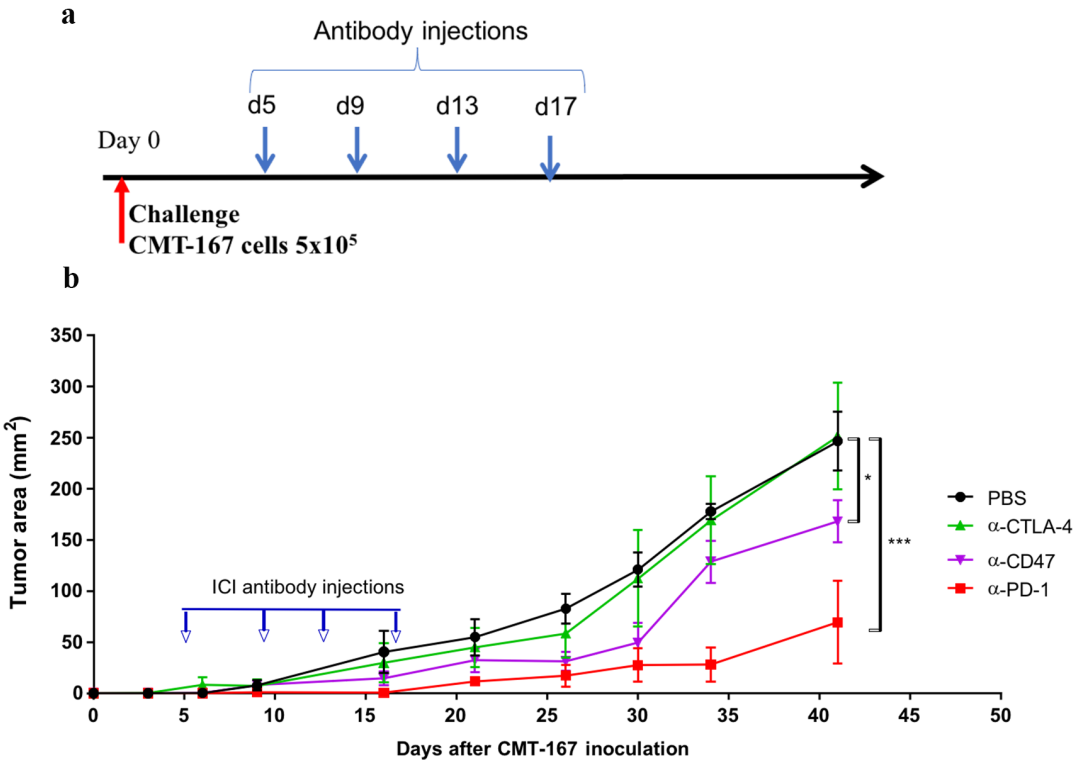

Figure 1. Anti-PD-1 antibody therapy reduces primary tumor growth of CMT-167 cells in mice. (a) Experimental schedule of anti-PD-1 antibody injections. Mice (n=5) were challenged with 5×10^5 cells on day 0 and then were given 4 doses of anti-PD-1/ anti-CTLA-4/ anti-CD47 antibodies every four days. (b) Tumor size was measured twice a week using calipers.

PROJECT I

MATERIALS AND METHODS

Cell culture

Mouse lung cancer CMT-167 cells were cultured in DMEM medium (Sigma Aldrich) supplemented with 10% BCS, 1% HEPES, 1% penicillin and streptomycin, 1% L-glutamine, and 0.1% gentamycin. To maintain the cell lines, the medium in the flasks was removed and 5 ml of trypsin was added to detach the adherent cells from the bottom of the T75 flasks. Then a volume of media was added to inactivate the trypsin and transferred it into a 15ml conical tube. The tube was centrifuged at 1200rpm for 5 minutes. After centrifugation, the supernatant was removed, and the pellet was dislodged by agitation. The the cells were resuspended in media and added $1/4^{th}$ back into the flask or expanded into new flasks for experiments. The flasks were kept in a 5% CO_2 incubator at 37°C and the cells were checked under a microscope on a daily basis.

IFN-γ treatment *in vitro*

For stimulation with IFN-γ, 5×10^5 CMT-167 cells were treated with 100ng/ml of recombinant mouse IFN-γ (Biolegend) in 3ml DMEM-complete medium in a 6-well plate. The cells were incubated in a 5% CO_2 incubator at 37°C for 72 hours. After 72 hours of incubation, the cells were harvested and stained with antibodies for flow cytometry analysis.

Tumor model and animals

C57BL/6 mice of 6–8 weeks age were purchased from The Jackson Laboratory (Bar Harbor, ME) and maintained in accordance with guidelines and protocols approved by the Institutional Animal Care and Use Committee (IACUC) of Emory University. For generation of CMT-167 tumors in C57BL/6 mice, 5×10^5 tumor cells in 100 µl PBS were injected subcutaneously (s.c.) in the hind flank of the mice. Mice were monitored for tumor growth every

3 days. Tumor size (mm^2) was measured using Vernier calipers. Mice were euthanized about 30 days after tumor challenge or if the longest dimension of the tumor reached 20mm before 30 days.

Prophylactic vaccination study

C57BL/6 mice were vaccinated s.c. with 2 doses of TMV vaccine (200 μg/ dose) in 100 μl PBS in the left hind flank on days 0 and 14. Blood samples were collected 6 days after vaccination for cytokine and antibody response analysis. Then mice were injected subcutaneously (s.c.) in the right hind flank with 5×10^5 CMT-167 cells on day 24. Tumor-free mice were subjected to a secondary challenge of 5×10^5 CMT-167 cells 4 months after the primary challenge. Mice were monitored for tumor growth every 3 days. At the IACUC end point, mice were euthanized to harvest lungs for metastasis assay.

Therapeutic vaccination study

For the therapeutic vaccination study, C57BL/6 mice were injected s.c. in the hind flank with 5×10^5 CMT-167 cells. Two doses of therapeutic TMV vaccination with 200 μg per dose were administered (s.c.) in the contralateral flank on days 3 and 10 after tumor challenge. Four doses of 200 μg anti-PD-1 antibody were administered intraperitoneally (i.p.) on days 3, 6, 10, and 13 post challenge. Mice were monitored as mentioned previously. At the end point, blood samples were collected for cytokine analysis and lungs were harvested for metastasis analysis.

***In vivo* cellular depletion**

CD4+ T cells, CD8+ T cells, and NK cells were depleted by i.p. injection of 200 μg of anti-CD4 (clone GK1.5), anti-CD8 (clone YTS 169.4), and anti-NK1.1 (clone PK136) antibodies in

dilution buffer. Cellular depletion was confirmed by flow cytometry analysis of CD4+ T cells, CD8+ T cells and NK cells in the blood samples within 24 hours after first dose of antibody injection. The next day, mice were challenged with 5×10^5 CMT-167 cells and another four doses of cellular depletion antibodies were given every four to five days post tumor challenge.

Cytokine assays

Blood samples from the submandibular vein were collected from the mice. The mice were anesthetized with isoflurane in an induction chamber. The facial vein was punctured with an animal lancet (5mm) and the blood samples were collected in a collection tube with 100 µl of Acid Citrate Dextrose (ACD) solution, which works as an anti-coagulant. After blood collection, a gauze sponge or an alcohol pad was used to stop the bleeding. The blood samples were then centrifuged to collect plasma. Cytokines present in circulation were detected in diluted plasma (1:10) using standard sandwich ELISA technique.

Enzyme-linked immunosorbent assay (ELISA)

To determine the presence of cytokines, a standard sandwich ELISA was performed. Briefly, 96-well ELISA plates were coated with capture antibody in coating buffer and incubated at 4°C overnight. Then the plates were washed three times with wash buffer (PBS-Tween20). After blocking for 2 hours with 1% BSA in PBS at room temperature, the plates were washed again three times with wash buffer. Then the plates were incubated with the samples and standards for 2 hours at room temperature, followed by three times of washing. The plates were incubated with biotinylated detection antibody for 1 hour at room temperature, followed by another three times of washing. Next, the plates were incubated with streptavidin-peroxidase for 30 minutes at room

temperature and washed five times with washing buffer. Then, the plates were incubated with TMB substrate for 30 minutes at room temperature. Finally, the reaction was stopped with 2M H_2SO_4 and the plates were read on a BioTek plate reader at 450 nm.

Lung metastasis assay

To quantify lung metastasis, a metastasis assay was performed. In a sterile environment, the lungs were harvested and placed in 1 ml HBSS in 35mm tissue culture dish. The lung tissue was minced using curved scissors and transferred to a 15ml conical tube. Then the minced lung tissue was incubated in 2ml of DMEM-complete media containing 1mg/ml freshly prepared collagenase type IV (Sigma) in shaking incubator at 37°C for 2 hours. After the 2-hour incubation, a single cell suspension was performed passing the digested lung tissue through a cell strainer. The tube was centrifuged, and the pellet was resuspended in 8ml selection media (800µg/ml G418 in DMEM-complete Medium for CMT-167 cells). After that, two sets were prepared from the stock lung cell suspension. In set I, 1ml of stock cell suspension diluted with another 3 ml of medium was plated in a 6-well plate in selection medium. After incubation for three days, the selection medium was removed, and DMEM-complete culture medium was added. Then the cells were checked under a microscope on a daily basis and when a single well of positive control reaches confluency, all the cells were harvested and counted using trypan blue to determine cell count and viability of the metastatic cells. In set II, the rest of the stock cell suspension was plated in selection medium in a 100mm tissue culture petri dish and selection medium were changed to culture medium after 3 days of incubation.

Cytotoxic T lymphocyte (CTL) assay

The TMVV-immunized mice were challenged with 5×10^5 CMT-167 tumor cells to activate the tumor antigen specific immune response in mice. Age-matched naïve mice were included as control. One week after tumor challenge, the spleens were harvested from the mice and single cell suspensions were prepared to collect the splenocytes. Red blood cells (RBSs) were lysed by adding 2 ml RBC lysis buffer with gentle agitation for 5 minutes. Cytotoxic T lymphocytes (CTLs) were expanded by co-culturing isolated splenocytes with mitomycin C-treated (50μg/ml) CMT-167 cells as stimulator cells at a 10:1 ratio for 7 days. Mouse recombinant IL-2 (10U/ml) was also added to stimulate T lymphocytes. After 7 days, dead cells were removed by using Lymphoprep (Stem Cell) centrifugation (2000rpm) for 30 minutes.

Next, cytotoxicity of T lymphocytes was measured by using the CytoTox 96 Non-radioactive Cytotoxic Assay (Promega). The target cells were prepared by treating CMT-167 cells with 100ng/ml mouse IFN-γ for 3 days to upregulate the level of MHC I and MHC II expressed on tumor cells. After that, CTLs were cultured with CMT-167 cells in a 96-well plate for at least 4 hours at 37 °C. Then, the supernatants of each well were transferred to a new 96-well plate and incubated with CytoTox 96 reagent for 30 minutes at room temperature to measure LDH release. Then stop solution was added and the plate was read to measure the absorbance signal at 490 nm in a BioTek plate reader. Finally, the percent cytotoxicity was calculated by using the following formula: $\%\ \text{Cytotoxicity} = \frac{\text{Experimental-Effector Spontaneous-Target Spontaneous}}{\text{Target Maximum-Target Spontaneous}} \times 100$

Cellular phenotyping of immune infiltrates

CMT-167 tumor cells were harvested and resuspended in 2 x 10^6 cells/ml in serum-free medium. 250μL of tumor cells (0.5 x 10^6) were mixed in a 1:1 ratio with 250μl of Matrigel

(Corning). The Matrigel-tumor cell mixture (500µl) was injected into the right hind flank of C57BL/6 mice. Mice injected with Matrigel with serum free medium (500µl) were included as control. Seven days after injection, the Matrigel was harvested and disintegrated by scalpels and forceps. Then single cell suspensions were prepared from Matrigel. Cells were washed three times with media and resuspended in FACS buffer for cell surface staining.

Flow cytometry

Cell surface receptors were analyzed by flow cytometry. Briefly, cells collected from *in vivo* studies were pre-incubated with Fc receptor blocking antibody in FACS buffer (PBS with 2% BCS, sodium azide 0.05%) at 4°C for 10 minutes to block nonspecific binding of monoclonal antibodies to immune cells. Then, cells were incubated with fluorochrome-conjugated primary antibodies for 30 minutes with shaking at 4°C. After that, the cells were washed three times with FACS buffer. Then the samples were fixed in 2% formaldehyde with PBS for later analysis or resuspended in FACS buffer for immediate analysis using a FACSCalibur or BD LSRII flow cytometer (BD Biosciences). Finally, data were analyzed using FlowJo (TreeStar Inc.) software.

BCA protein assay

A Pierce BCA protein assay kit (Thermo Scientific) was used to quantify the protein content in the TMVs and TMVVs. In a U-bottom 96 well plate, 25µl of each standard and sample replicate was added to the plate. Then 200µl of the BCA working reagent was added to each well. After mixing the plate thoroughly with a plate shaker, the plate was incubated at 37°C for 30 minutes. After incubation, the plate was read at 562nm on a BioTek plate reader to measure the absorbance.

Statistical analysis

All the statistical analyses and graphs were performed using GraphPad Prism software. Significance of mean differences was determined by using two-tailed paired or unpaired student t-tests or two -way ANOVA test. Values of $p<0.05$ were considered significant ($*p < 0.05$, $**p < 0.01$, $***p \leq 0.001$). Survival curves were plotted and analyzed using Kaplan-Meier analysis.

PROJECT I

RESULTS

Prepare and verify incorporation of GPI-ISMs onto TMVs

To develop personalized immunotherapy vaccine, we prepared tumor membrane vesicles (TMVs) from tumor tissue and modified the TMVs with immunostimulatory molecules (ISMs) by protein transfer to make TMV vaccine (TMVVs). First, C57BL/6 mice were challenged with 5 x 10^5 CMT-167 cells and the tumor tissue samples were harvested at the IACUC end point. Then tumor tissue samples were homogenized three times with a tissue homogenizer, followed by one hour of sucrose gradient ultracentrifugation to get TMVs in the interface (Fig. 2a). Next, the TMVs were collected and washed with 1xPBS three times. The resulting TMVs were 300 to 500 nm in size and a representative Scanning Electron Microscopic (SEM) image was shown (Fig. 2b). Finally, TMVs were incubated with glycosylphosphatidylinositol (GPI)- linked IL-12 and B7-1 (Metaclipse Therapeutics Corporation, Atlanta) for 4 hours at 37°C to generate TMVVs (Fig. 2a). The total concentration of protein in the TMVs and TMVVs was determined by a microBCA protein assay (Thermo Scientific). Incorporation of GPI-IL-12 and GPI-B7-1 molecules onto TMVs was confirmed by flow cytometry analysis (Fig. 2c).

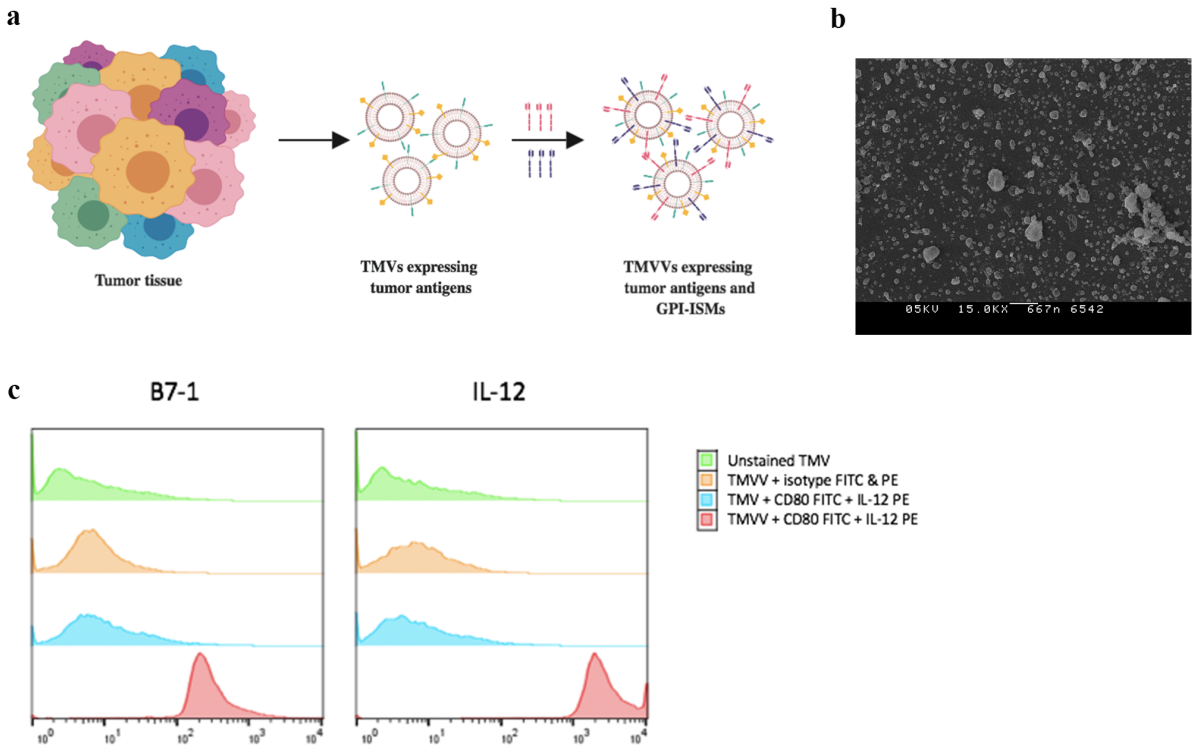

Figure 2. Tumor membrane vesicles (TMVs) preparation and incorporation of immunostimulatory molecules (ISMs) on the TMVs via a GPI-anchor to form TMV vaccine (TMVVs). (a) Schematic representation of TMVV preparation. First, tumor tissue with a wide range of clonal populations is homogenized and TMVs were collected by sucrose gradient ultracentrifugation. Second, TMVs are incubated with GPI-IL-12 and GPI-B7-1 for 4 hrs at 37°C to generate TMV vaccine (TMVVs). (b) A representative SEM image of TMVs prepared from tumor tissue. (c) The expression of GPI-IL-12 and GPI-B7-1 on TMVVs was indicated by flow cytometry analysis.

Characterization of CMT-167 TMVs

Surface antigens on CMT-167 cells were determined by flow cytometry. CMT-167 cells were cultured in DMEM-complete medium under standard condition and flow cytometry analysis was performed to determine certain surface markers expressed on the cells. The specific markers that were analyzed include MHC I, MHC II, CD24, CD44, CD49d, ICAM-1, CD47, PD-L1, CD80, and CD86. Among these markers, we found that CMT-167 cells express CD24, CD44, CD47, and PD-L1 *in vitro* (Fig. 3a, b). Next, after CMT-167 TMVs were generated, I have performed flow

cytometry to analyze the same markers again. The results show that in addition to these four markers that CMT-167 cells express *in vitro*, CMT-167 TMVs also express MHC I, MHC II, and ICAM-1 (Fig. 3d, e). To investigate if the expression of MHC I, MHC II, and ICAM-1 markers on tumor tissue-derived TMVs is induced by IFN-γ in the tumor microenvironment, I have treated CMT-167 cells (0.5 x 10^6) with 100ng/ml of IFN-γ for 72 hours. Then the IFN-γ-treated cells were harvested for flow cytometry analysis. I found that stimulation with IFNγ upregulates the level of MHC I, MHC II, ICAM-1, and PD-L1 on CMT-167 cells (Fig. 3a, c).

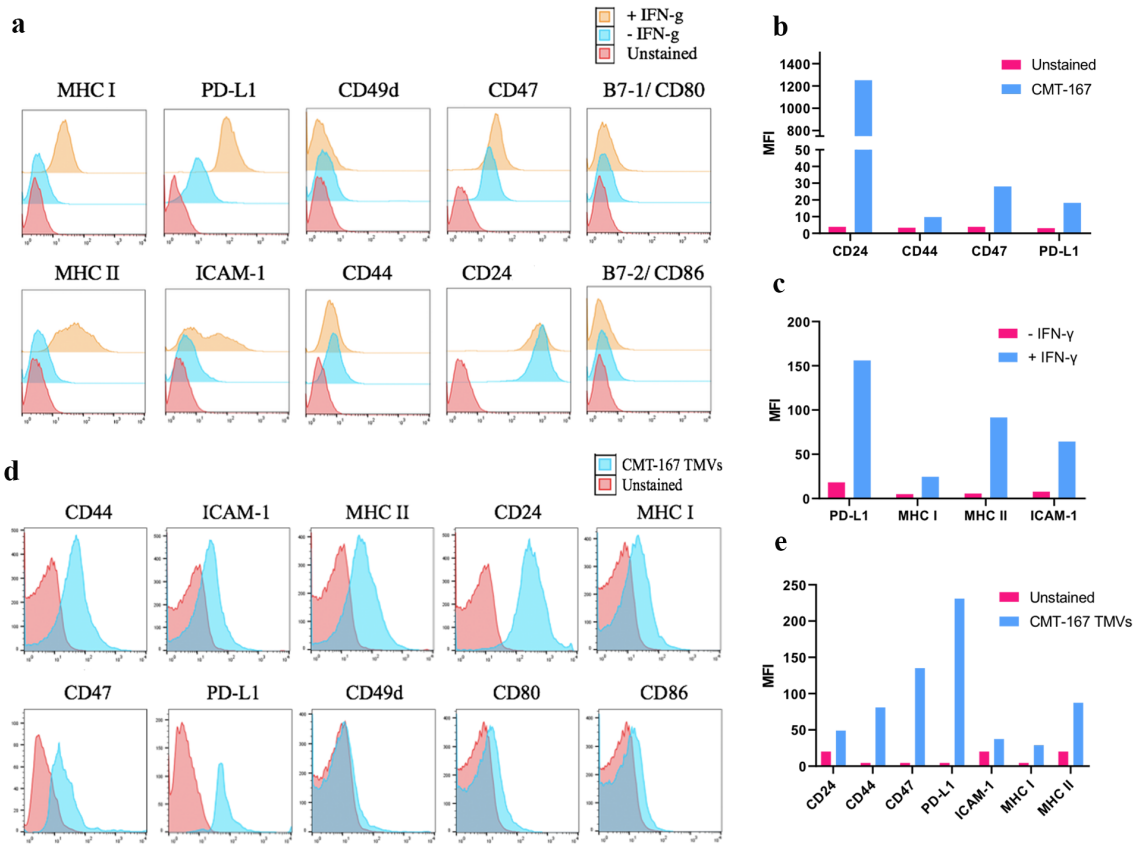

Figure 3. Surface markers of CMT-167 cells and TMVs (a) Flow cytometry analysis of cell surface antigens of CMT-167 cells in culture with or without IFN-γ treatment. (b) CMT-167 cells express CD24, CD44, CD47, and PD-L1 *in vitro*. (c) IFN-γ treatment elevates the levels of MHC I, MHC II, ICAM-1, and PD-L1 expression on CMT-167 cells in culture. (d) Flow cytometry

analysis of surface markers on CMT-167 TMVs. (e) CMT-167 TMVs express CD24, CD44, CD47, PD-L1, MHC I, MHC II, and ICAM-1.

Prophylactic TMVV immunotherapy prolongs the survival and induces immunological memory in CMT-167-tumor bearing mice

To investigate the efficacy of TMVVs in protecting mice against tumor cell challenge, we first conducted a prophylactic vaccination study using CMT-167 tumor model in C57BL/6 female mice. Mice were given 2 doses of TMVs or TMVVs on Day 0 and 14 into one flank and were challenged with 5 x 10^5 tumor cells s.c. in the opposite flank (Fig. 4a). The tumor size of the mice was monitored every 3 days. We observed that 80% of the mice vaccinated with TMVVs and 20% of mice vaccinated with TMVs were protected against tumor cell challenge. The tumor-free survival rate of TMVV-vaccinated mice is significantly higher than the control mice (Fig. 4b). Four months after the first tumor challenge, these five tumor-free mice were then re-challenged with 5 x 10^5 CMT-167 tumor cells (Fig. 4c). Most of the mice were still protected by the prophylactic TMV or TMVV immunotherapy against CMT-167 cells, which is indicated by the result that 80% of the mice remained tumor-free after the re-challenge (Fig. 4d). These data indicate that the prophylactic vaccination of TMVV or TMV protects mice from CMT-167 tumor cell challenge and helps mice develop immunological memory to eradicate tumors upon tumor re-challenge.

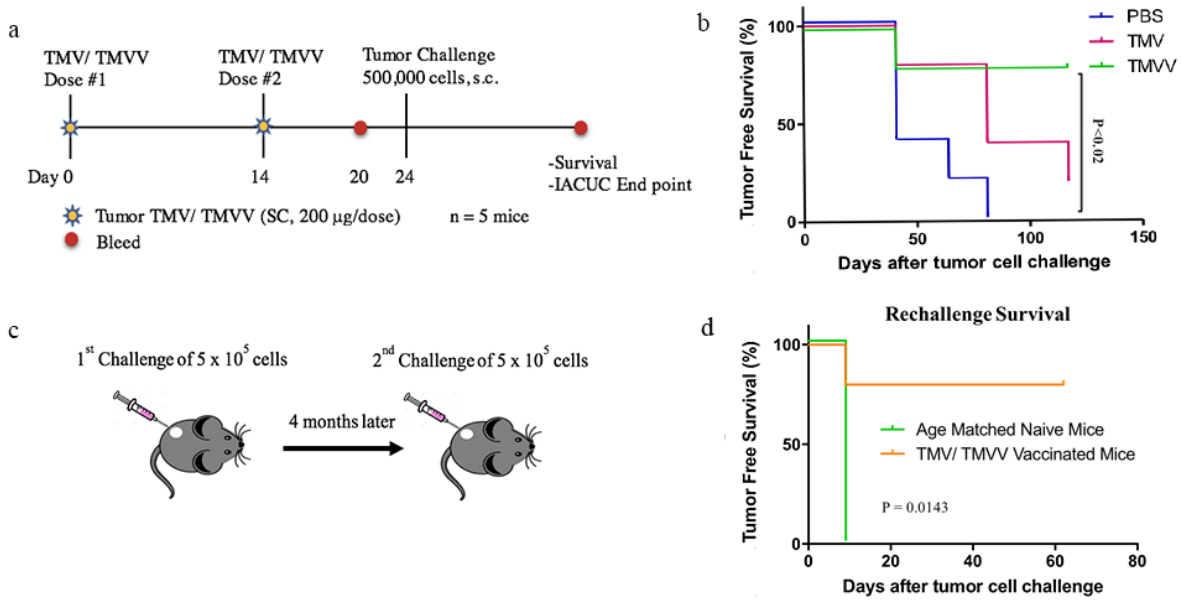

Figure 4. Prophylactic TMV or TMVV immunotherapy prolongs the survival and induces immunological memory in CMT-167-tumor bearing mice. (a) Experimental schedule of prophylactic TMV/ TMVV immunotherapy study. C57BL/6 mice (n=5) were immunized with 200 µg TMV or TMVV s.c. in the flank on days 0 and 14, followed by inoculation with $5x10^5$ CMT-167 cells s.c. in the contralateral flank on day 24. (b) Tumor-free survival curve after primary tumor cell challenge is shown. (c) Tumor-free mice were subjected to a second challenge with 5 x 10^5 cells 4 months after the first tumor cell challenge. Age-matched naïve mice (n=5) were included as control. (d) Tumor-free survival of the mice after re-challenge is shown.

Therapeutic TMVV immunotherapy inhibits CMT-167 primary and metastatic tumor growth

Next, we performed a therapeutic vaccination study using the same CMT-167 metastatic tumor model in C57BL/6 mice to determine if the TMVV immunotherapy inhibits primary tumor growth and lung metastasis effectively in a therapeutic setting. Since we have observed the upregulation of PD-L1 by IFN-γ on the CMT-167 tumors, we also investigated whether the combination of immune checkpoint inhibitor (ICI) therapy using anti-PD-1 antibodies, with TMVV immunotherapy could further boost tumor specific immune response in mice. In this study, mice were inoculated s.c. with 5 x 10^5 tumor cells on Day 0 and treated with two doses of TMVV

immunotherapy on d3 and d10 days after tumor challenge. Then, mice were injected with four doses of anti-PD-1 antibodies twice a week after tumor challenge (Fig. 5a). We observed that tumor progression was significantly inhibited in mice treated with TMVV immunotherapy (Fig. 5b) and primary tumor regression in 40% of mice were observed (Fig. 5c). At the IACUC end point, mice were euthanized, lung tissue was harvested, and single cell suspensions were prepared. The cells were then cultured in a 6-well plate and G418 (800μg/ml) was used to inhibit the fibroblasts. The remaining tumor cells were cultured for 1 to 2 weeks and then counted to quantify the metastatic lung cells. We found that TMVV immunotherapy significantly reduced the metastatic tumor burden (Fig. 5d). Interestingly, anti-PD-1 antibody alone didn't protect mice from tumor challenge and combing anti-PD-1 antibody with TMVV immunotherapy didn't have a synergistic or additive effect on the primary or metastatic tumor growth (Fig. 5b-d).

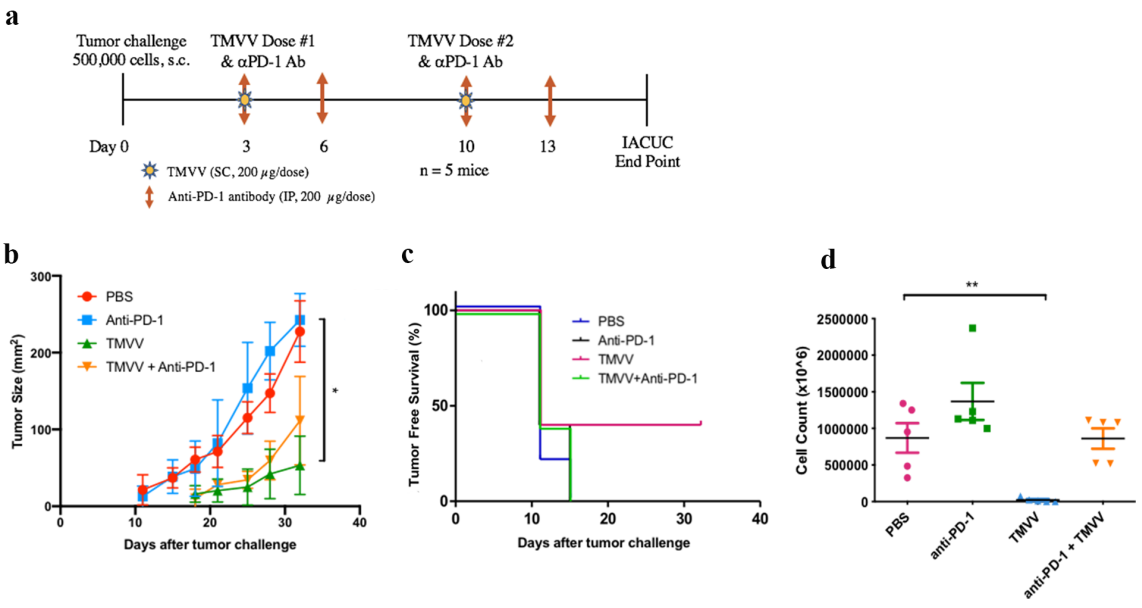

Figure 5. Therapeutic vaccination of TMVV inhibits CMT-167 tumor growth and significantly reduces lung metastasis. (a) Experimental design of therapeutic immunotherapy study. C57BL/6 mice (n=5) were challenged with 5×10^5 CMT-167 cells s.c. in the flank on day 0 and treated with 2 doses of TMVV immunotherapy on days 3 and 10. Mice were also administered with 4 doses of 200 μg anti-PD-1 antibody i.p. on days 3, 6, 10, and 13 post tumor

challenge (b) Tumor growth curves and (c) percent tumor-free survival of the mice with different treatments is shown. (d) Lungs were collected from the mice and single cell suspensions were prepared. Then the cells were treated with G418 (800μg/ml) in 6-well plates for 3 days to inhibit fibroblasts and then cultured in fresh media to detect lung metastasis. Cells were counted when a single well reached confluency.

CD4+ T cells, CD8+ T cells, and NK cells are involved in anti-tumor effect induced by prophylactic TMVV immunotherapy in CMT-167-tumor bearing mice

So far, our findings show that prophylactic vaccination of TMV adjuvanted with immunostimulatory molecules prevents the CMT-167 tumor growth in mice and helps the mice develop immunological memory to the tumor challenge, while therapeutic TMVV vaccination inhibits tumor growth and significantly reduces the metastatic tumor burden. To investigate the mechanism of TMVV immunotherapy-induced immune response in mice, we conducted an *in vivo* cell depletion study in a prophylactic setting to assess the relative roles of CD4+ T cells, CD8+ T cells, or NK cells. Following two doses of TMVV immunotherapy, mice were depleted of CD4+ T cells, CD8+ T cells, or NK cells by administration of cell depletion antibodies (200μg/ dose). Blood samples were collected within 24 hours of the first dose of cellular depletion antibodies to confirm the efficacy of depletion. After confirmation, mice were challenged with 5 x 10^5 tumor cells s.c. and injected with another four doses of cell depletion antibodies every 4 to 5 days to deplete newly formed lymphocytes (Fig 6a).

Compared to the positive control group (TMVV-vaccinated mice), cellular depletion of CD4+ T cells and NK cells compromised the protective effect of prophylactic TMVV immunotherapy at the early stage. By 30 days after tumor challenge, the mice depleted of CD4+ T cells and NK cells as well as the PBS control mice had severe tumor burden and thus were euthanized (Fig. 6b-c). The tumor-free mice were kept further monitoring. Interestingly, tumor growth in CD8+ T cells depleted TMVV-vaccinated mice was significantly reduced and percent

of tumor-free survival of these mice was significantly increased at the beginning. However, tumors appeared after a long dormancy in all but one mouse from this group (Fig. 6b, c). These results indicate that both CD4+ T cells and NK cells are required for efficacy of anti-tumor response induced by the prophylactic TMVV immunotherapy, while CD8+ T cells provide help for an increased effect of TMVV-induced cellular immunity. At the IACUC end point for tumor burden, mice were sacrificed and lung tissue samples were harvested to assess metastatic tumor growth. We observed that in spite of CD4+ T cells or NK cells depletion, the lung metastasis of mice in these two groups was still significantly lower compared to the PBS control (Fig. 6d). This suggests that CD8+ T cells alone are sufficient to control lung metastasis and the presence of CD4+ T cells (mice with NK cell depletion) effectively inhibits metastatic tumor growth in lungs by prophylactic TMVV immunotherapy in mice.

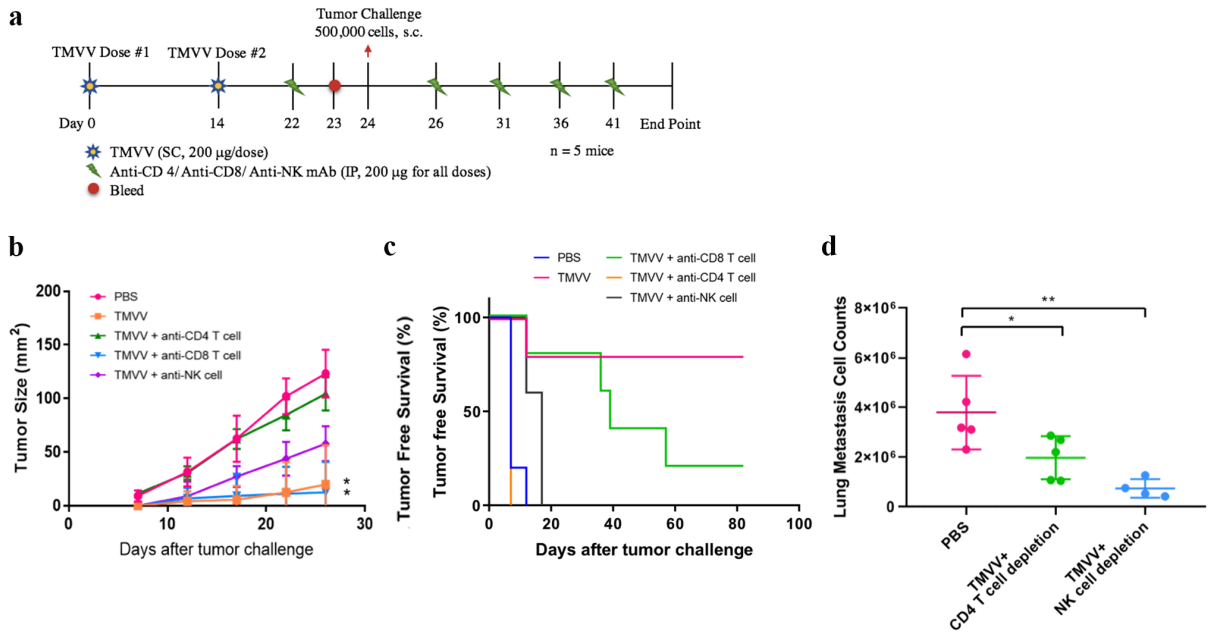

Figure 6. CD4+ T cells, CD8+ T cells, and NK cells are involved in the anti-tumor response induced by the TMV vaccine immunotherapy. (a) Experimental design of cellular depletion study in a prophylactic setting. C57BL/6 mice (n=5) were immunized with 2 doses of TMV vaccine (200 µg) s.c. in the flank, followed by the first dose (200 µg) of antibodies to deplete CD4+ T cells, CD8+ T cells, or NK cells one week after vaccination. Blood samples were collected within 24 hours to confirm the efficacy of depletion. Then the mice were challenged with $5x10^5$

tumor cells s.c. and injected i.p. with another four doses of cellular depletion antibodies every 5 days. (b) Tumor growth and (c) percent tumor-free survival of the mice are shown. (d) At the IACUC end point (d28), vaccinated mice with depletion of CD4+ T cells and NK cells, as well as the PBS control group were euthanized, while vaccinated mice with or without CD8+ T cell depletion were surviving. The lung tissue was collected from the euthanized mice and single cell suspensions were prepared. The cells were treated with G418 (800μg/ml) in 6-well plates for 3 days to inhibit fibroblasts and then cultured in fresh media to detect lung metastasis. Cells were counted when any one well reached confluency.

TMVV immunotherapy induces robust CTL activities

To further investigate the roles of CD4+ T cells, CD8+ T cells and NK cells in TMVV-mediated cellular immunity, we assessed the level of cytotoxic T lymphocyte (CTL) activities of splenocytes from TMVV-vaccinated mice survived from the previous cellular depletion study. First, to confirm IFN-γ secretion in tumor microenvironment upon TMVV vaccination, spleens were harvested from the TMVV-vaccinated mouse and age-matched naïve mouse. After preparing single cell suspensions, splenocytes were plated in a 48-well plate pre-coated with anti-CD3 (2ug/ml) and TMVV (50ug/ml) overnight. The plate was incubated at 37 °C for 24 hours and then the supernatants were collected for ELISA analysis. The results show that TMVV immunotherapy induces *in vitro* IFN-γ secretion in splenocytes from TMVV-immunized mice (Fig. 7a).

Next, a CTL assay was conducted to measure LDH release using the CytoTox 96 Non-radioactive Cytotoxic Assay (Promega). TMVV-immunized mice were re-challenged with 5 x 10^5 CMT-167 cells to activate immune response. Seven days after re-challenge, spleens were harvested and splenocytes were prepared and stimulated with mitomycin-treated CMT-167 cells for 7 days. Then the activated CTLs were incubated with IFN-γ-treated CMT-167 target cells for at least 4 hours at E:T ratios of 10:1, 5:1, and 2.5:1. We observed that splenocytes from TMVV-immunized mice are capable to kill approximately 60% of CMT-167 target cells at an E:T ratio of 10:1, which is significantly higher than the splenocytes from age-matched naïve mice (Fig. 7b).

To assess the specificity of cytotoxic activity of CD4+ or CD8+ T cells, we used anti-CD4 or anti-CD8 antibodies in the co-culture. Our data show that prophylactic TMVV-mediated CTL activities were compromised if either CD4+ or CD8+ T cells were blocked (Fig. 7c).

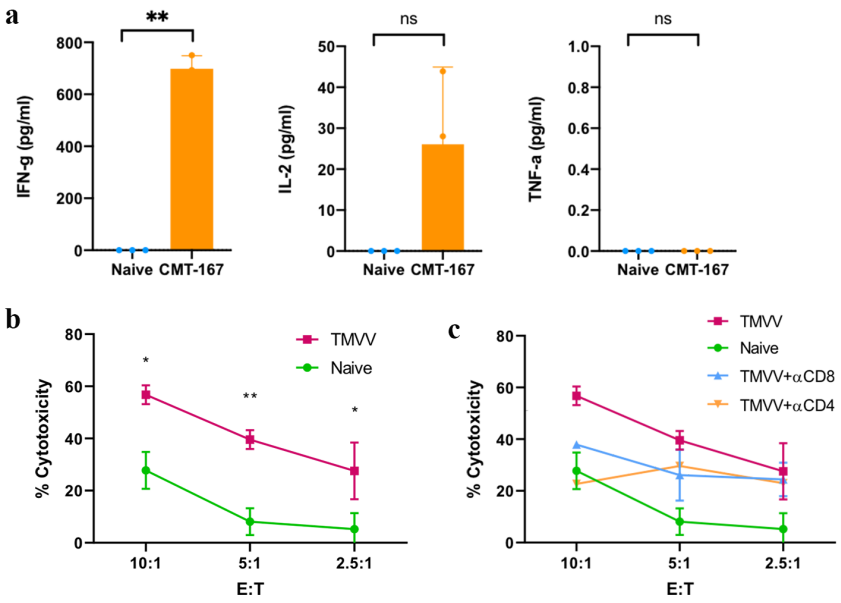

Figure 7. Induction of tumor antigen specific CTL response in the mice immunized with TMV vaccine that survived from CMT-167 tumor challenge. (a) Stimulation of splenocytes with TMVV immunotherapy induces IFN-y secretion. (b-c) TMVV-immunized mice and age-matched control mice (n=2) were re-challenged with 5 x 10^5 CMT-167 cells. Splenocytes were collected from mice seven days after re-challenge and expanded *in vitro* for seven days with mitomycin-treated CMT-167 cells at an effector: target (E:T) ratio of 10:1. Then CTLs were incubated with IFN-γ-treated CMT-167 target cells for at least 4 hours at the indicated E:T ratios. Cytotoxicity of T lymphocytes was measured by LDH release using the CytoTox 96 Non-radioactive Cytotoxic Assay (Promega).

TMVV immunotherapy alters the tumor microenvironment of the CMT-167 tumors

To gain insight into the specific immune factors mediated by prophylactic TMVV immunotherapy, CMT-167 tumor cells were mixed with Matrigel in a 1:1 ratio, and the mixture was transplanted s.c. into the TMVV-immunized mice survived from previous cellular depletion study. Two types of control are included: age-matched naïve mouse injected with Matrigel alone and age-matched naïve mouse injected with Matrigel-tumor cells mixture. Seven days after the

inoculation, Matrigel was harvested and single cell suspension was prepared from Matrigel, followed by flow cytometry analysis. We observed that TMVV immunotherapy induces both CD4+ and CD8+ T cell infiltration in tumor tissue. However, more activated CD4+ T cells are found in the tumor microenvironment indicated by an increase in granularity (Fig. 8a). Moreover, in the CD45- population, there are more MHC II+ cells in the naïve mouse than in the TMVV-immunized mouse after injection of Matrigel-tumor cells mixture. Then we looked at the percentage of CD45- cells, which indicate non-hematopoietic cells, we found more CD45- cells in the naïve mouse than in the TMVV-immunized mouse injected with Matrigel-tumor cells mixture (Fig. 8a). This suggests that there are less MHC II-expressing tumor cells in the mice vaccinated with TMVV immunotherapy compared to the naïve control. Therefore, it's possible that TMVV immunotherapy can induce MHC II-restricted CD4+ T cell-mediated killing of target cells.

To further investigate how CD4+ T cells render cytotoxic activities to eradicate tumor cells, we assessed the level of eosinophils (CD11b+, Siglec F+) and macrophages (F4/80+, CD206+) in the tumor microenvironment since previous research has shown that CD4+ T cells, in addition to be helper T cells, can also secrete granulocyte/ macrophage colony stimulating factors to activate eosinophils and microphages to eradicate tumor cell challenge[11]. Our FACS data show that TMVV immunotherapy induces infiltration of both eosinophils and macrophages (Fig. 8b). Interestingly, we observed that TMVV immunotherapy induces more MDSC in the tumor microenvironment, which can be explained by the active activity of tumor cells that are trying to establish immunosuppressive microenvironment to escape immune surveillance (Fig. 8b). Overall, these results indicate that MHC II-restricted CD4+ T cells probably play a role in anti-tumor immunity induced by prophylactic TMVV immunotherapy by recruiting eosinophils and macrophages in the tumor site to eradicate the tumor cells.

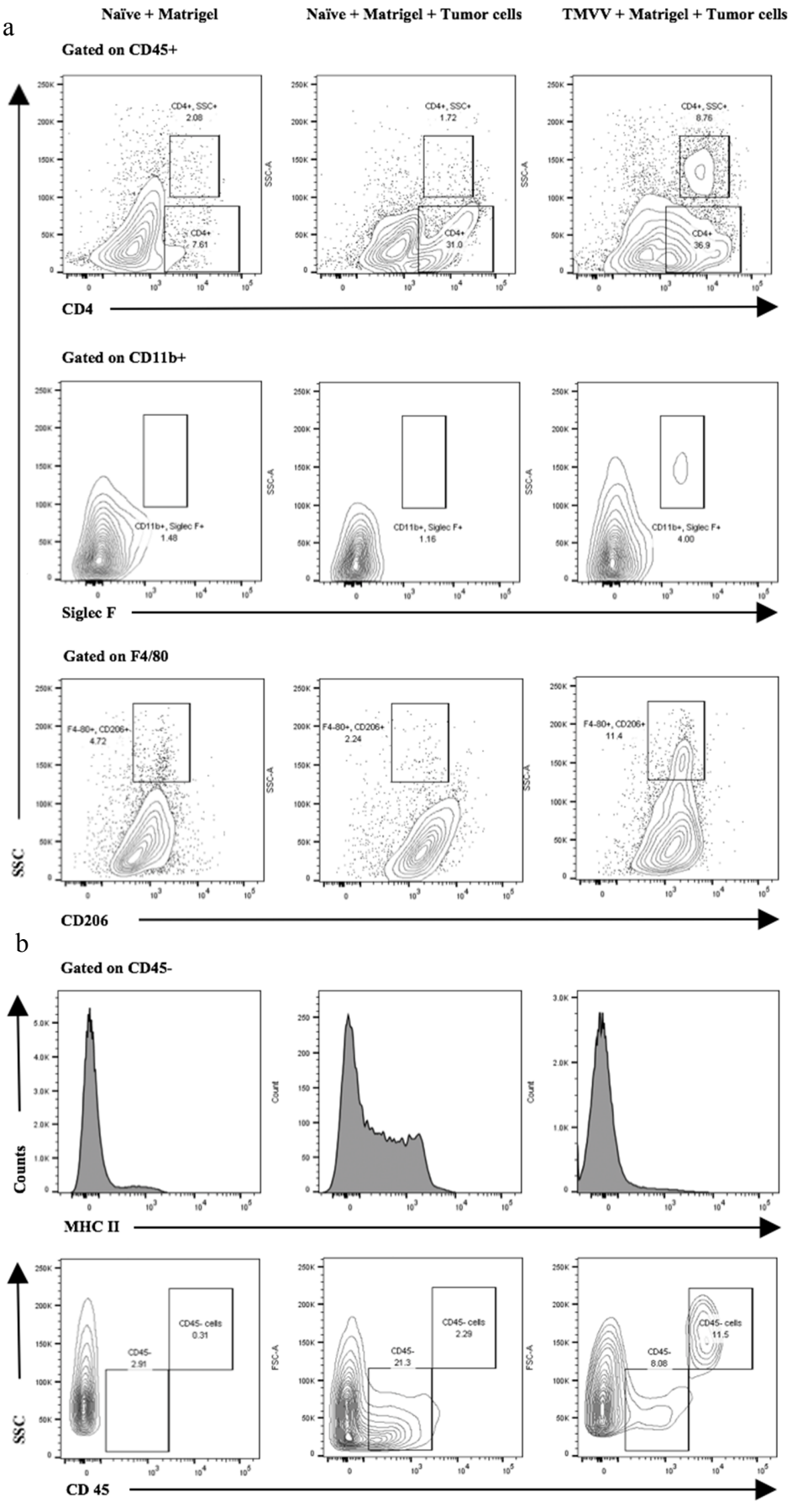
a
Naïve + Matrigel
Naïve + Matrigel + Tumor cells
TMVV + Matrigel + Tumor cells
Gated on CD45+
CD4+, SSC+
2.08
CD4+
7.61
CD4+, SSC+
1.72
CD4+
31.0
CD4+, SSC+
8.76
CD4+
36.9
SSC-A
CD4
Gated on CD11b+
CD11b+, Siglec F+
1.48
CD11b+, Siglec F+
1.16
CD11b+, Siglec F+
4.00
Siglec F
Gated on F4/80
F4-80+, CD206+
4.72
F4-80+, CD206+
2.24
F4-80+, CD206+
11.4
SSC
CD206
b
Gated on CD45-
Counts
Count
MHC II
CD45- cells
0.31
CD45-
2.91
CD45- cells
2.29
CD45-
21.3
CD45- cells
11.5
CD45-
8.08
FSC-A
CD 45

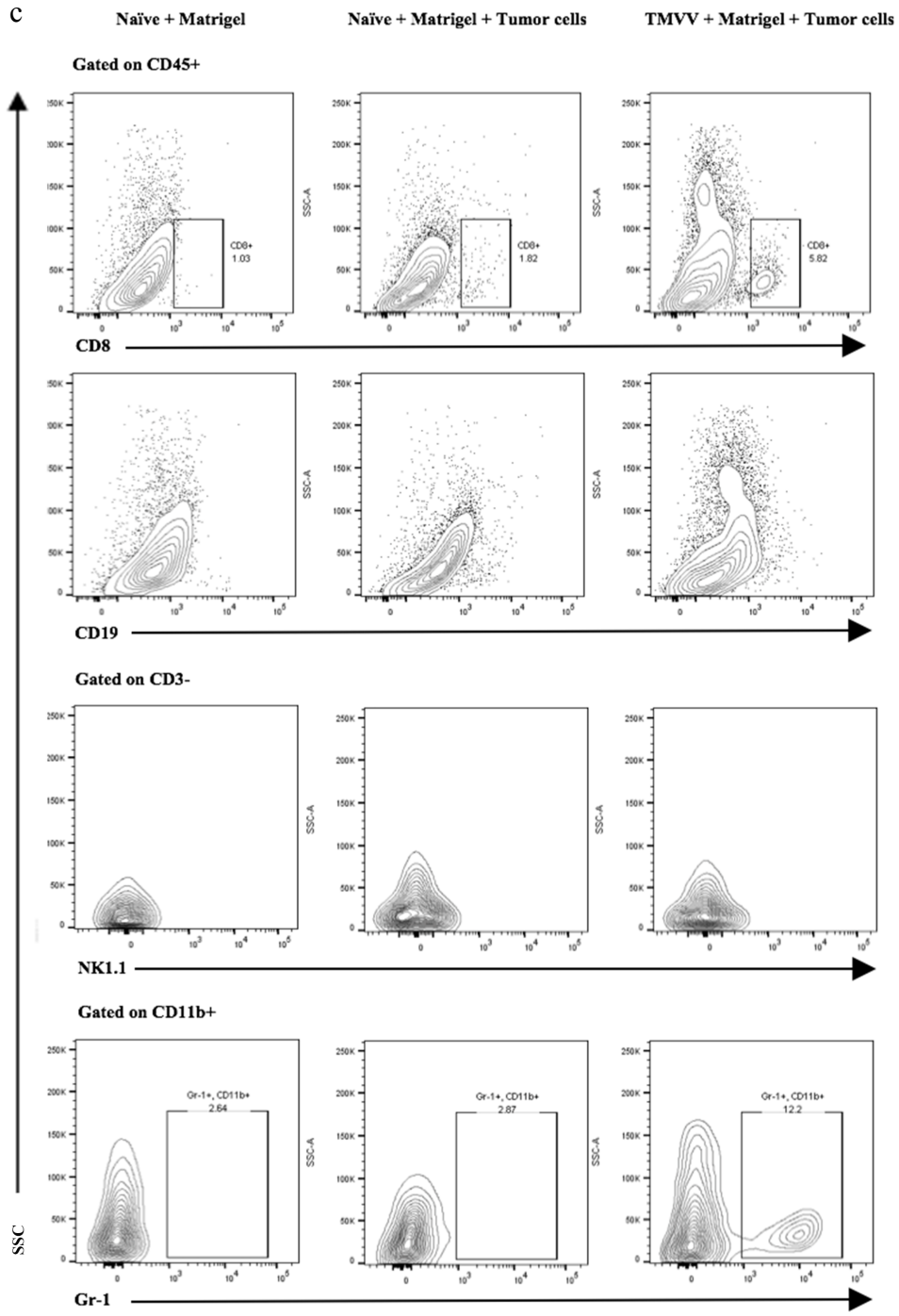

Figure 8. Prophylactic TMVV immunotherapy induces MHC II-restricted CD4 T cell-mediated killing of CMT-167 tumor cells by activation of eosinophils and macrophages in tumor microenvironment. (a) FACS plot of CD4 T cells (CD45+, CD4+), eosinophils (CD11b+, Siglec F+), and macrophages (F4/80+, CD206+). (b) Flow plots of MHC II+ tumor cells (top) and population of CD45- tumor cells (bottom). (c) Flow plots of CD8 T cells (CD45+, CD8+), B cells (CD45+, CD19+), NK cells (CD3-, NK1.1+), and MDSC (Gr-1+, CD11b+) in tumor microenvironment.

PROJECT I

DISCUSSION

We demonstrate that prophylactic vaccination of TMV adjuvanted with GPI-IL-12 and GPI-B7-1 prevents the CMT-167 tumor growth in mice and induces immunological memory to the tumor cell challenge. In a therapeutic setting, we find that TMVV vaccination induced regression of primary tumor in 40% of the mice and significantly reduced the metastatic tumor burden. However, the combination of TMVV vaccination with anti-PD-1 mAb doesn't have a synergistic or additive effect on the primary or metastatic tumor growth. Surprisingly, anti-PD-1 mAb therapy failed to inhibit CMT-167 tumor growth in this study, which is in contrast with our previous study (Fig. 1). Thus, the experiments are being repeated to test the efficacy of anti-PD-1 antibodies. We are also planning to determine the effect of other ICI therapies and the combination of these ICI therapies with TMV vaccine in the CMT-167 cancer model.

Moreover, our study offers a rationale for developing personalized TMVV immunotherapy for MHC II-expressing tumor model to stimulate MHC II-dependent CD4+ T cells-mediated cytotoxic activity. CD8+ T lymphocytes, which are classic killer T cells are dispensable in TMVV-mediated cellular immunity in this model. However, CD8+ T lymphocytes play a significant role in enhancing the effect of TMVV vaccination. This is indicated by the results of cellular depletion study, in which TMVV-immunized mice remained tumor-free for one month but tumor formation was observed in majority of the mice within the next two months.

Furthermore, the Matrigel experiment suggests that TMVV immunotherapy induces accumulation of eosinophils and macrophages to the tumor site. Previous studies have shown that CD4+ T cells can secrete granulocyte/ macrophage colony stimulating factors to activate eosinophils and microphages to eradicate the tumors[11]. Therefore, future experiments are needed to assess the level of granulocyte/ macrophage colony stimulating factors in the tumor microenvironment such as G-CSF, GM-CSF, and etc. Furthermore, it is also shown that

macrophages which produce superoxide and nitric oxide can synergize with eosinophils which express peroxidase to eradicate tumor cells effectively[11]. Therefore, in our studies, it's possible that the collaboration of macrophages and eosinophils induced by CD4 T cells contribute to the anti-tumor immune response. Hence, more experiments are needed to assess the production of superoxide, nitric oxide, and eosinophil peroxidase in the tumor microenvironment. Finally, the Matrigel experiment to investigate cellular phenotyping of immune infiltrates is needed to be repeated to confirm the results. Overall, these studies provide insight into using the immunotherapy of TMV adjuvanted with membrane-anchored ISMs for treating the partially ICI resistant lung cancer.

REFERENCES

1. Dela Cruz, C.S., Tanoue, L.T. & Matthay, R.A. Lung cancer: epidemiology, etiology, and prevention. *Clin Chest Med* **32**, 605-644 (2011).

2. Siegel, R.L., Miller, K.D. & Jemal, A. Cancer statistics, 2019. *CA Cancer J Clin* **69**, 7-34 (2019).

3. Esposito, L., Conti, D., Ailavajhala, R., Khalil, N. & Giordano, A. Lung Cancer: Are we up to the Challenge? *Curr Genomics* **11**, 513-518 (2010).

4. Gadgeel, S.M., Ramalingam, S.S. & Kalemkerian, G.P. Treatment of lung cancer. *Radiol Clin North Am* **50**, 961-974 (2012).

5. Grigg, C. & Rizvi, N.A. PD-L1 biomarker testing for non-small cell lung cancer: truth or fiction? *J Immunother Cancer* **4**, 48 (2016).

6. Nagarajan, S. & Selvaraj, P. Glycolipid-anchored IL-12 expressed on tumor cell surface induces antitumor immune response. *Cancer Res* **62**, 2869-2874 (2002).

7. Leonard, J.P. *et al.* Effects of single-dose interleukin-12 exposure on interleukin-12-associated toxicity and interferon-gamma production. *Blood* **90**, 2541-2548 (1997).

8. Chen, L. & Flies, D.B. Molecular mechanisms of T cell co-stimulation and co-inhibition. *Nat Rev Immunol* **13**, 227-242 (2013).

9. Trinchieri, G. & Scott, P. Interleukin-12: basic principles and clinical applications. *Curr Top Microbiol Immunol* **238**, 57-78 (1999).

10. Franks, L.M., Carbonell, A.W., Hemmings, V.J. & Riddle, P.N. Metastasizing tumors from serum-supplemented and serum-free cell lines from a C57BL mouse lung tumor. *Cancer Res* **36**, 1049-1055 (1976).

11. Hung, K. *et al.* The central role of CD4(+) T cells in the antitumor immune response. *J Exp Med* **188**, 2357-2368 (1998).

PROJECT II

Expression of red fluorescent protein increases TILs while inhibits tumor-induced G-CSF and MDSC in a fully ICI resistant murine lung cancer model

INTRODUCTION

Cancer immunotherapy has become a promising approach in treating lung cancer patients recently[12]. The discovery of immune checkpoint inhibitor (ICI) therapy is a breakthrough in cancer immunotherapy. In the programmed cell death-1 (PD-1) pathway, the usage of anti-PD-1 or anti-PD-L1 antibodies can block the interaction of PD-1 on T cells with its ligands, PD-L1 or PD-L2, expressed on tumor cells, which allows cytotoxic T cells to kill the tumor cells[13]. Various studies have shown that PD-L1 is upregulated in non-small cell lung cancer (NSCLC), which suggests a potential effectiveness of ICI therapy in NSCLC patients[5]. Despite impressive ICI treatment outcomes in a subset of NSCLC patients, majority of the patients fail to respond to ICI therapy[5].

In this study, we studied a fully ICI-resistant murine lung cancer model to gain an insight into possible mechanism of ICI resistance in NSCLC patients. The lung cancer model that we studied is Lewis Lung Carcinoma (LL/2), which is derived spontaneously from lung carcinoma of C57BL/6 mice by J.S. Bertram in 1951[14]. Our previous studies have demonstrated that LL/2 tumors are highly tumorigenic and ICI therapy or the combination of ICI therapy with other immunotherapy, including tumor membrane vesicles (TMVs) and MPL adjuvant could not induce anti-tumor immunity in the LL/2 tumor model (Fig. 1). However, we accidently found that LL/2 cells labeled with red fluorescent protein (RFP) become immunogenic.

To investigate the effect of transfection with a foreign antigen, RFP on LL/2 tumor cells, we first compared the morphologic features of both cell lines by flow cytometry to analyze the cell surface markers, and then we conducted *in vivo* mice study to examine the immunogenic effect of RFP expression. Since several studies have reported that the efficacy of cancer immunotherapy is negatively correlated with increased MDSC level[15], we assessed the level of MDSC in spleen, tumor, and blood samples as well as the MDSC-inducing factors in the blood from mice challenged with LL/2 or LL/2-RFP cells. To further investigate the role of anti-tumor immune cells in RFP-

mediated immunity, an *in vivo* cell depletion study was conducted. Finally, we also tested whether transfection with RFP induces a more robust anti-tumor immunity in response to tumor membrane vesicle (TMV) immunotherapy, which is a personalized vaccine immunotherapy prepared from individual tumor tissue. Overall, our studies demonstrate that transfection of a fully ICI resistant murine cancer model with RFP induces tumor immunogenicity by increasing tumor infiltrating lymphocytes (TILs) while inhibiting tumor induced MDSC levels.

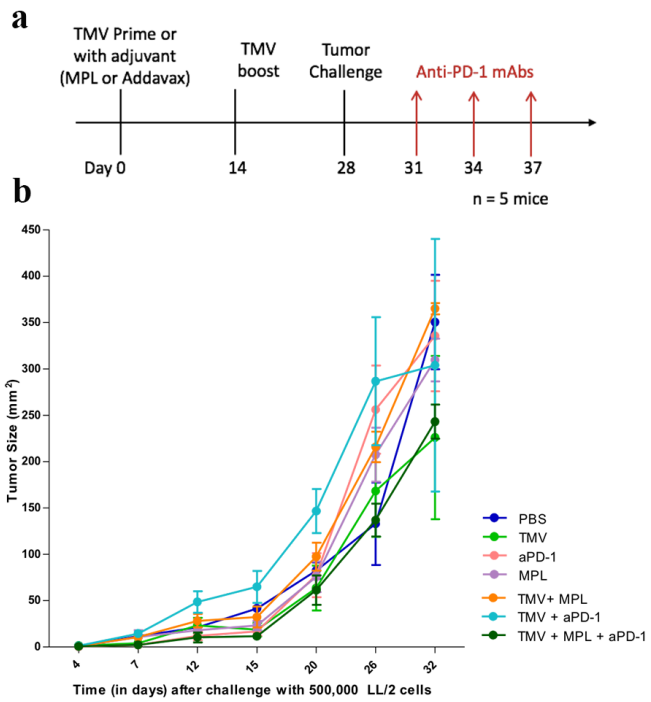

Figure 1. Immunotherapy of TMV, MPL adjuvant, anti-PD-1 antibody, or their combinations do not protect against LL/2 tumor in mice. (a) Experimental schedule of immunotherapy. C57BL/6 mice (n=5) were injected with TMV vaccine alone or with adjuvant (MPL or Addavax) and were given a booster dose after 2 weeks. Two weeks after the booster dose, $5x10^5$ LL/2 cells were inoculated s.c. in to the flank. Three days after the tumor cell challenge, anti-PD-1 (200 μg/mouse) antibody was injected i.p. for a total of three doses with 3 days apart. (b) Tumor growth was monitored, and tumor size was shown.

PROJECT II

MATERIALS AND METHODS

Cell culture

Mouse lung cancer LL/2 and LL/2-RFP cells were cultured in DMEM medium (Sigma Aldrich) supplemented with 10% fetal bovine serum (FBS), 1% HEPES, 1% penicillin and streptomycin, 1% L-glutamine, and 0.1% gentamycin. To maintain the cell lines, the medium in the flasks was removed and 5 ml of trypsin was added to detach the adherent cells from the bottom of the T-75 flasks. Then a volume of media was added to inactivate the trypsin in a 15ml conical tube. The tube was centrifuged at 1200rpm for 5 minutes. After centrifugation, the supernatant was removed, and the pellet was dislodged by agitation. Then the cells were resuspended in media and added back into the flask. The flask was kept in a 5% CO_2 incubator at 37°C and the cells were checked under a microscope on a daily basis.

Cell proliferation assay

To measure cell proliferation *in vitro*, LL/2 or LL/2-RFP cells were harvested and resuspended in DMEM-complete medium. Then 1×10^5 cells were plated in a T-25 flask in 3-5 ml medium on day 0. The cells were cultured in a 5% CO_2 incubator at 37°C for 3 days and were harvested for counting by using trypan blue to determine the cell count and cell viability. Then all the cells were transferred to a T-75 flask for continued culturing for another 3 days. On day 6, the cells were harvested and counted again.

IFN-γ treatment *in vitro*

For stimulation with IFN-γ, 5×10^5 LL/2 or LL/2-RFP cells were treated with 100ng/ml of recombinant mouse IFN-γ (Biolegend) in 3ml DMEM-complete medium using a 6-well plate. The cells were incubated in a 5% CO_2 incubator at 37°C for 72 hours. After 72 hours of incubation,

cells were harvested for flow cytometry analysis, and supernatants were collected for cytokine analysis by ELISA.

Single cell cloning

LL/2-RFP cells were harvested and resuspended in DMEM-complete medium at a concentration of 100 cells/ 10ml. The cells were mixed thoroughly. Then 100μl of the resuspended cells was added to each well of a 96-well plate. Ideally, each well should contain one cell. The plates were incubated in a 5% CO_2 incubator at 37 °C and were monitored on a daily basis to check the cell clone development. When a clone developed, it was first transferred to a 48-well plate, then to a 24-well plate, finally to a 6-well plate for culturing. After enough cells from a single clone were established, the cells were harvested to check the expression of RFP by flow cytometry analysis.

Tumor model and animals

C57BL/6 mice of 6–8 weeks age were purchased from The Jackson Laboratory and maintained in accordance with guidelines and protocols approved by the Institutional Animal Care and Use Committee (IACUC) of Emory University. For growing LL/2 or LL/2-RFP tumors in C57BL/6 mice, 5×10^5 cells were injected subcutaneously (s.c.) in the flank of the mice. Mice were monitored for tumor growth every 3 days. Tumor size (mm^2) was measured using Vernier calipers. Mice were euthanized about 30 days after tumor challenge or if the longest dimension of the tumor reached 20mm before 30 days.

Prophylactic vaccination study

C57BL/6 mice (n=5) were vaccinated s.c. with 2 doses of TMV vaccine (200 μg/ dose) in the left hind flank on days 0 and 14. Then mice were injected subcutaneously (s.c.) in the right hind flank with 5×10^5 LL/2 or LL/2-RFP cells on day 24. At the IACUC end point, mice were euthanized to harvest lungs for metastasis assay, tumors and spleens for flow cytometry analysis, and blood samples for cytokine and MDSC analysis.

***In vivo* cellular depletion**

CD4+ T cells, CD8+ T cells, and NK cells were depleted by i.p. injection of 200 μg of anti-CD4 (clone GK1.5), anti-CD8 (clone YTS 169.4), and anti-NK1.1 (clone PK136) antibodies in dilution buffer. Cellular depletion was confirmed by flow cytometry analysis of CD4+ T cells, CD8+ T cells and NK cells in the blood samples within 24 hours after first antibody injection. The next day, mice were challenged with 5×10^5 LL/2 or LL/2-RFP cells and another four doses of cellular depletion antibodies were given every four to five days post tumor challenge to deplete newly formed lymphocytes.

Cell preparation from various organs or tissues

At the IACUC end point, mice were euthanized. Spleen and tumor tissue were harvested and placed in 1ml of PBS in a 35mm tissue culture dish. The tumor tissue was minced using curved scissors or scalpels. Then the minced tumor tissue was transferred to a 15 ml conical tube and incubated in 2ml of freshly prepared DMEM-complete media containing 1mg/ml collagenase type IV (Sigma), 10% DNase (Invitrogen) and 10% Liberase (Roche) in a shaking incubator at 37°C for at least 30 minutes. After digestion, single cell suspensions were prepared by mechanical

disruption of the tissue and passage through a cell strainer. Then the cell strainer was rinsed with PBS. The tube was centrifuged, and the cell pellet was resuspended in PBS and was ready for counting and flow cytometry analysis.

To prepare murine splenocytes, the spleens were disrupted using the back of a syringe plunger to pass through a cell strainer directly after tissue harvesting. Then the splenocytes were incubated with red blood cell (RBC) lysis buffer (5ml/ spleen) at room temperature for 5 minutes with occasional shaking for removing the RBCs. The cells were washed with PBS and were counted and used for flow cytometry analysis.

Lung metastasis assay

To quantify metastatic cells to the lungs, a lung metastasis assay was performed. In a sterile environment, the lungs were harvested and placed in 1 ml of HBSS in a 35mm tissue culture dish. The lung tissue was minced using curved scissors and transferred to a 15ml conical tube. Then the minced lung tissue was incubated in 2ml of freshly prepared DMEM-complete media containing 1mg/ml collagenase type IV (Sigma) in a shaking incubator at 37°C for 2 hours. After the 2-hour incubation, single cell suspensions were performed by passing the digested lung tissue through a cell strainer. The cells were centrifuged, and the pellet was resuspended in 8ml selection media (400μg/ml G418 in DMEM-complete Medium for LL/2 or LL/2-RFP cells). After that, two sets were prepared from the stock lung cell suspension. In set I, 1ml of stock cell suspension was plated in a 6-well plate in selection medium. After incubation for three days, the selection medium was removed, and DMEM-complete culture medium was added. Then the cells were checked under a microscope on a daily basis and when one of the wells reaches confluency, all the cells were harvested and counted using trypan blue to determine cell count and viability of the metastatic

cells. In set II, the rest of the stock cell suspension was plated in selection medium in a 100mm tissue culture petri dish and selection medium were changed to culture medium after 3 days of incubation.

Cytokine assays

Blood samples from the submandibular vein were collected from the mice. The mice were anesthetized with isoflurane in an induction chamber. The facial vein was punctured with an animal lancet (5mm) and the blood samples were collected in a collection tube with 100 µl of Acid Citrate Dextrose (ACD) solution, which works as an anti-coagulant. After blood collection, a gauze sponge or an alcohol pad was used to stop the bleeding. The blood samples were then centrifuged to collect plasma. Cytokines present in circulation were detected in diluted plasma (1:10) using standard sandwich ELISA technique.

Cytokine production in cell culture was measured by growing LL/2 or LL/2-RFP cells at a concentration of 10^6 cells/ 4 ml in a 6-well tissue culture plate. The plate was incubated in a 5% CO_2 incubator at 37°C for 48 hours. After incubation, cell culture supernatants were harvested and analyzed for cytokines by ELISA technique. Specifically, we determined the presence of the following cytokines: TNF-alpha, TGF-beta, IL-6, GM-CSF, G-CSF, VEGF, and IFN-gamma.

Enzyme-linked immunosorbent assay (ELISA)

To determine the presence of cytokines, a standard sandwich ELISA was performed. Briefly, 96-well ELISA plates were coated with capture antibody in coating buffer and incubated at 4 °C overnight. Then the plates were washed three times with wash buffer (PBS-Tween). After blocking for 2 hours with 1% BSA in PBS at room temperature, the plates were washed again three

times with wash buffer. Then the plates were incubated with the samples and standards for 2 hours at room temperature, followed by three times of washing. The plates were incubated with biotinylated detection antibody for 1 hour at room temperature, followed by another three times of washing. Next, the plates were incubated with streptavidin-peroxidase for 30 minutes at room temperature and washed five times with washing buffer. Then, the plates were incubated with TMB substrate for 30 minutes at room temperature. Finally, the reaction was stopped with 2M H_2SO_4 and the plates were read on BioTek plate reader at 450 nm.

Flow cytometry

Cell surface receptors were analyzed by flow cytometry. Briefly, cells collected from *in vivo* studies were pre-incubated with Fc receptor blocking antibody in FACS buffer (PBS with 2% BCS, sodium azide 0.05%) at room temperature for 10 minutes to block nonspecific binding of monoclonal antibodies to immune cells, while cells from culture doesn't need to be Fc blocked. Then, cells were incubated with fluorochrome-conjugated primary antibodies for 30 minutes with shaking at 4°C. After that, the cells were washed three times with FACS buffer. Then the samples were fixed in 2% formaldehyde with PBS for later analysis or resuspended in FACS buffer for immediate analysis using a FACSCalibur or BD LSRII flow cytometer. Finally, data were analyzed using FlowJo (TreeStar Inc.) software.

For cell sorting, cells were harvested using trypsin to detach cells from the bottom of the flask and were resuspended in DMEM-complete medium at a concentration of 1×10^7 cells/ ml. Cell sorting was performed by pediatrics flow cytometry core facility in the Health Sciences Research Building of Emory University. The top 20% of RFP positive cells and the bottom 10% of RFP negative cells were selected to establish pure LL/2 and LL/2-RFP cell lines.

Statistical analysis

All the statistical analyses and graphs were performed using GraphPad Prism software. Significance of mean differences was determined by using two-tailed paired or unpaired student t-tests or two -way ANOVA test. Values of $p<0.05$ were considered significant ($*p < 0.05$, $**p < 0.01$, $***p \leq 0.001$). Survival curves were plotted and analyzed using Kaplan-Meier analysis.

PROJECT II

RESULTS

Cloning and verification of RFP expression in LL/2-RFP NEG and LL/2-RFP POS cells

To clone LL/2 and LL/2-RFP cells, a single cell cloning and a cell sorting were performed. In the single cell cloning method, single LL/-RFP cells from original culture were isolated in each well of a 96-well plate to establish clones. Then each proliferating clone was transferred to a 48-well plate, then a 24-well plate, finally a 6-well plate for culturing. After enough cells from a single clone were established, the cells were harvested to check the expression of RFP by flow cytometry analysis. In the cell sorting, original LL/2-RFP cells were harvested and sorted using flow cytometry. The top 20% of RFP positive (POS) cells and the bottom 10% of RFP negative (NEG) cells were selected to establish a pure LL/2 and LL/2-RFP cell lines. After sorting, the cells were cultured in T-75 flasks under standard condition for 7 days and then harvested to verify for their RFP expression by flow cytometry. The population with the highest purity was selected to expand in T175 flasks and then frozen to create a cell stock. The FACS plot of RFP expression in the selected LL/2-RFP NEG and LL/2-RFP POS cell lines is shown (Fig. 2a).

Next, to determine if the RFP expression is stable *in vivo*, I have inoculated LL/2 and LL/2-RFP cell lines in C57BL/6 mice. Mice were challenged with 2×10^5 LL/2-RFP POS cells s.c. in the flank. Then the tumor size was monitored every 3 days. At the IACUC end point, the tumor and lung tissues were collected and analyzed by flow cytometry for RFP expression. LL/2-RFP cells in tumor and lung tissues maintained the RFP expression *in vivo* (Fig. 2b).

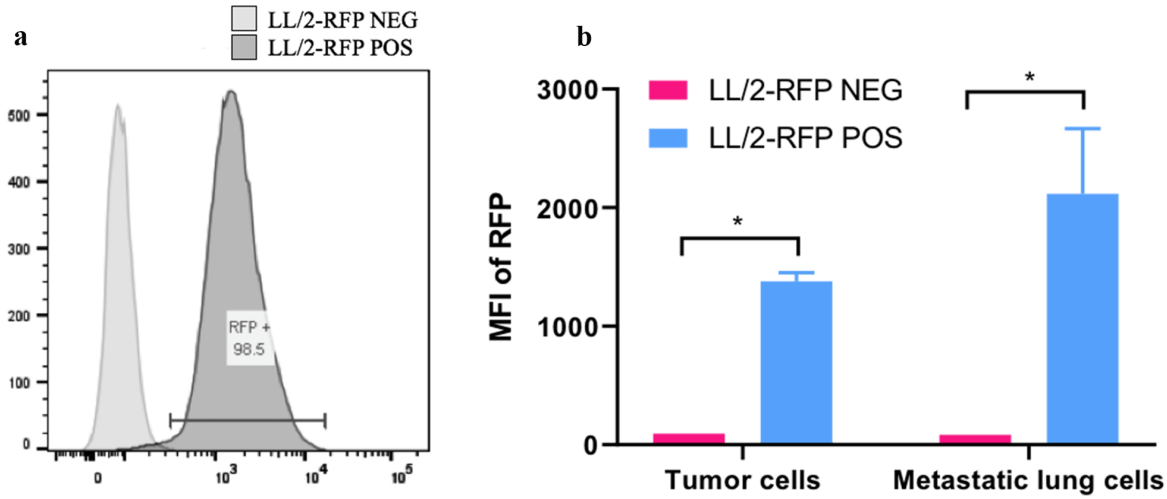

Figure 2. RFP expression is maintained *in vivo*. (a) FACS plot of RFP expression of the selected LL/2-RFP negative (NEG) and LL/2-RFP positive (POS) cell lines with the highest purity. (b) Mice (n=3) were challenged with 2×10^5 LL/2-RFP POS cells s.c. in the flank. At the endpoint, the tumor and lung tissues were collected and analyzed for RFP expression.

Surface antigens of LL/2 and LL/2-RFP cells in culture

After cloning the LL/2 and LL/2-RFP cells, we checked the cell surface markers by flow cytometry. The specific markers that we checked include MHC I, MHC II, CD24, CD44, CD49d, ICAM-1, CD47, PD-L1, CD80, and CD86. Among these markers, both cell lines express CD44, CD47, as well as PD-L1 (Fig. 3a) and the MFI of these antigens are similar between the two cell lines (Fig. 3b). This demonstrates that aside from the RFP-modification, these cell lines are morphologically comparable. Next, we also treated LL/2 and LL/2-RFP cells with IFN-γ to assess the potential changes in antigen expression of tumor cells *in vivo*. Five hundred thousand cells were treated with 100ng/ml of IFN-γ at 37°C for 72 hours. Then the IFN-γ-treated cells were harvested for flow cytometry analysis. We found that stimulation with IFNγ upregulates the level of MHC I, MHC II, and PD-L1 in both types of cells (Fig. 3c-e). Therefore, except for RFP-

expression, LL/2 and LL/2-RFP have the same membrane morphology with or without IFN-γ treatment.

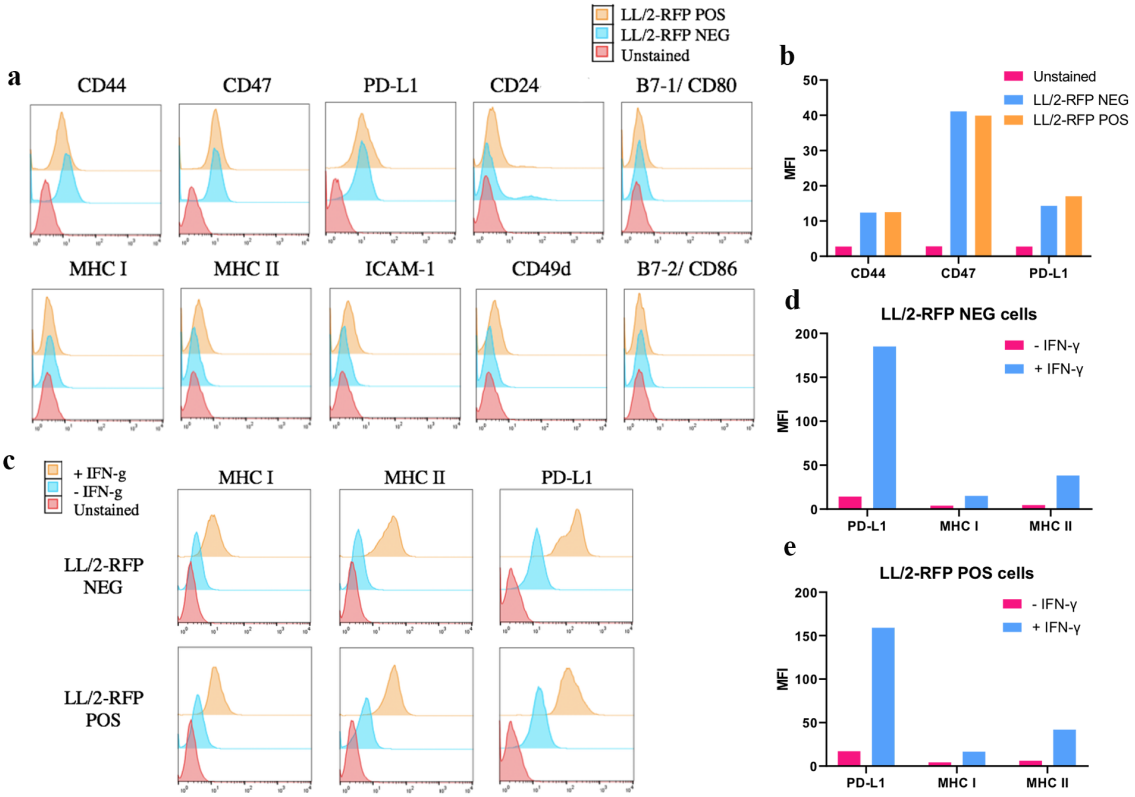

Figure 3. Cell surface markers of LL/2-RFP NEG and POS cells. (a) Flow cytometry analysis of surface markers of LL/2-RFP NEG and POS cells. They both express CD44, CD47, and PD-L1 in culture. (b) MFI of antigen expression in two cell lines. (c) IFN-g treatment (100ng/ml for 72 hours) elevates the level of MHC I, MHC II, and PD-L1 expression in both LL/2-RFP NEG and POS cells. (d-e) MFI of antigen expression in two cell lines after IFN-γ treatment.

Transfection with RFP expression inhibits tumorigenicity of LL/2 tumor cells

To investigate the effect of RFP expression in LL/2 tumor model on its tumorigenicity, a simple tumor challenge study was conducted. C57BL/6 mice were challenged with 5×10^5 cells s.c. in the flank and the tumor growth was monitored every three days. Mice were euthanized at the IACUC endpoint and the spleens, tumors, and blood samples from facial vein were collected (Fig. 4a). We observed that LL/2-RFP tumors grow slower than LL/2 tumors *in vivo* (Fig. 4b). To

exclude the possible effect of a difference in cell proliferation, we assessed the cell growth potential of the two cell lines *in vitro*. 1×10^5 LL/2 or LL/2-RFP cells were plated in a T-25 flask on day 0 and are counted on day 3 and 6. Our data show that LL/2-RFP cells grow at a faster rate compared to LL/2 cells *in vitro* (Fig. 4c). Since LL/2-RFP cells proliferate faster than parental LL/2 cells *in vitro*, their decreased growth *in vivo* is likely due to a better immune response against LL/2-RFP tumors than LL/2 tumors. Moreover, the spleen weight of LL/2-RFP-tumor bearing mice was significantly smaller than that of LL/2-tumor bearing mice (Fig. 4d). Previous studies have shown that the spleen is a predominant feature of many pathological conditions and massive splenomegaly (spleen enlargement) is associated with malignancy and poor prognosis[16, 17]. Therefore, this study indicates that the RFP expression in LL/2 cell line inhibits its tumorigenicity as indicated by slower tumor growth and smaller spleen size in LL/2-RFP tumor model compared to LL/2 model.

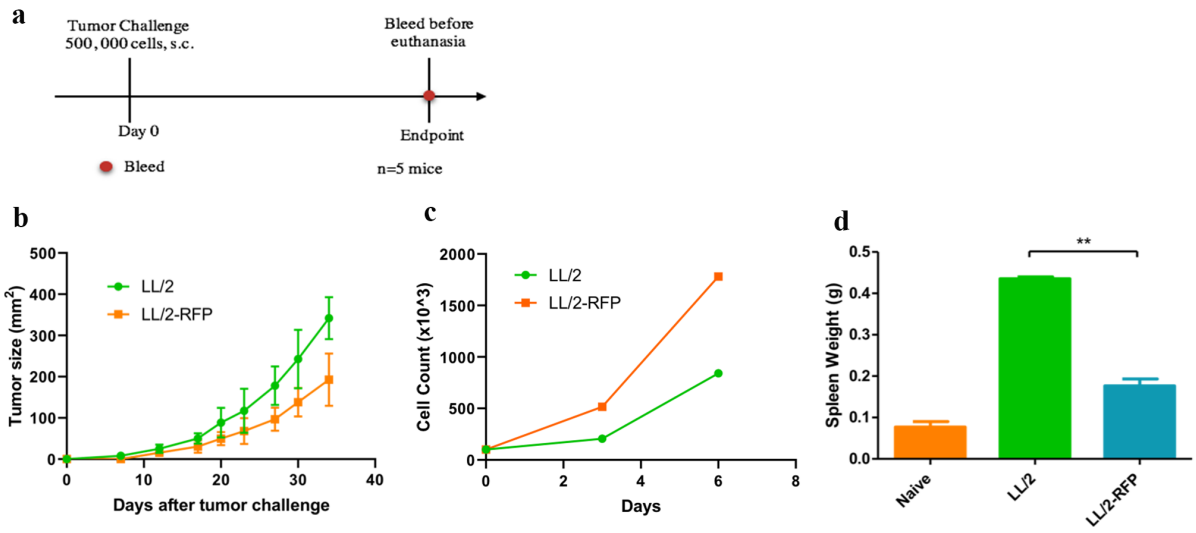

Figure 4. RFP expression in LL/2 cells inhibits its tumorigenicity. (a) Experimental design of direct tumor challenge study. C57BL/6 mice (n=5) were challenged with 5×10^5 cells s.c. in the flank and the tumor growth was monitored every three days. Mice were euthanized at the IACUC endpoint and the spleens, tumors, and blood samples from facial vein were collected. (b) LL/2 tumors grow faster than LL/2-RFP tumors *in vivo*, (c) LL/2 cells grow slower than LL/2-RFP cells *in vitro*. (d) Spleen weight of LL/2-RFP tumor bearing mice is significantly smaller compared to LL/2 tumor bearing mice.

The expression of RFP in LL/2 cells induces tumor immunogenicity by inhibiting tumor induced G-CSF and MDSC levels

To test the hypothesis that the decreased growth of LL/2-RFP cells *in vivo* is due to a better immune response against LL/2-RFP tumors, tumor infiltrating lymphocytes (TILs) were analyzed by flow cytometry. We found that there are significantly more CD4+ T cells (CD45+, CD3+, CD4+), CD8+ T cells (CD45+, CD3+, CD8+), and B cells (CD45+, CD3+, CD19+) infiltration in LL/2-RFP tumors compared to LL/2 tumors (Fig. 5a-c). Since myeloid-derived suppressor cells (MDSC) are precursor myeloid cells with immunosuppressive and tumorigenic capabilities[18], we also assessed the level of MDSC (Gr-1+, CD11b+) in blood, spleen and tumor samples by flow cytometry analysis. Compared to the LL/2-tumor bearing mice, LL/2-RFP-tumor bearing mice have significantly lower level of MDSC in blood and tumor tissue (Fig. 5d-f). This result confirms the previous observation that the RFP expression induces tumor immunogenicity by inhibiting immunosuppressive MDSCs.

Furthermore, we have determined the cytokine secretion in plasma and cell culture supernatants to check whether LL/2 tumors secrete more MDSC-inducing factors than LL/2-RFP tumors *in vivo*. Numerous studies have demonstrated that immunosuppressive functions of MDSC was upregulated by inflammatory molecules such as IFN-γ, G-CSF, GM-CSF, VEGF, IL-6, IL-1β, TNF-α, COX-2, etc[19]. Among these MDSC-inducing factors, we have analyzed the secretion of cytokines G-CSF, GM-CSF, TNF-α, IL-6, IL-1β, and IFN-γ in plasma by ELISA. Our data show that the level of cytokines GM-CSF, TNF-α, IL-6, IL-1β, and IFN-γ was not detectable (Fig. 5g), so they are not likely contributing to the increase in MDSCs. However, we observed that the secretion of G-CSF is significantly increased in plasma derived from LL/2-tumor bearing mice compared to LL/2-RFP-tumor bearing mice (Fig. 5h). To confirm that the increased G-CSF level

in plasma is due to immune cells *in vivo*, we assessed the secretion of G-CSF by LL/2 and LL/2-RFP cells *in vitro*. 4T1 breast cancer cells were included as control since 4T1 cells are known to secrete G-CSF which induces MDSCs[20]. Compared to the positive control, the 4T1 cells, no G-CSF level was detected from the supernatants collected from LL/2 and LL/2-RFP cell culture (Fig. 5i). Therefore, these data indicate the elevated level of G-CSF in the plasma of LL/2-tumor bearing mice may contribute to increased MDSCs while RFP transfection of LL/2 cells induce TILs and inhibit inhibiting tumor induced G-CSF and MDSC levels.

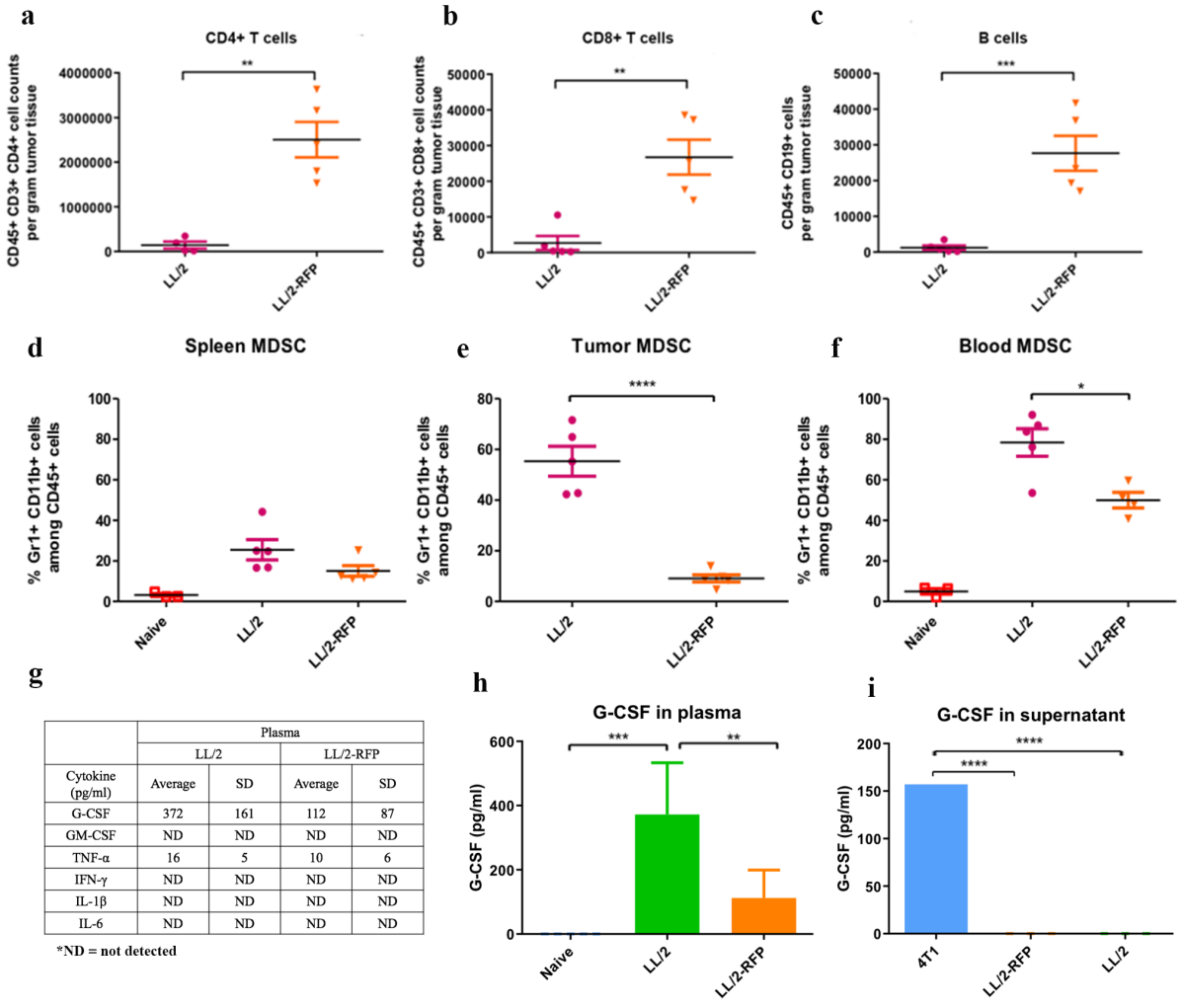

	Plasma			
	LL/2		LL/2-RFP	
Cytokine (pg/ml)	Average	SD	Average	SD
G-CSF	372	161	112	87
GM-CSF	ND	ND	ND	ND
TNF-α	16	5	10	6
IFN-γ	ND	ND	ND	ND
IL-1β	ND	ND	ND	ND
IL-6	ND	ND	ND	ND

*ND = not detected

Figure 5. The expression of RFP in LL/2 cells induces tumor immunogenicity by inhibiting tumor induced G-CSF and MDSC levels. (a-c) More CD4+ T cells, CD8+ T cells, and B cells infiltration in LL/2-RFP tumors compared to LL/2 tumors. (d-f) MDSC levels of tumor and blood

are significantly reduced in LL/2-RFP tumor bearing mice compared to LL/2. (g) GM-CSF, TNF-α, IL-6, IL-1β, and IFN-γ cytokines are probably not accounted for inducing MDSC levels in LL/2-tumor bearing mice (n=5). (g-i) G-CSF is increased in the plasma of LL/2-RFP tumor bearing mice, but not in culture.

LL/2-RFP tumor growth is inhibited by CD4+ T cells, CD8+ T cells, and NK cells *in vivo*

To further investigate whether anti-tumor immune cells are involved in the decreased level of G-CSF production in LL/2-RFP-tumor bearing mice, an *in vivo* cell depletion study was conducted. C57BL/6 mice were depleted of CD4+ T cells, CD8+ T cells, or NK cells by i.p. injection of cellular depletion antibodies (200μg/ dose). Blood samples were collected within 24 hours of the first dose of cellular depletion antibodies to confirm the efficacy of depletion. After confirmation, mice were challenged with 5×10^5 cells s.c. in the flank and subsequently injected with another four doses of cellular depletion antibodies every five days to deplete newly formed lymphocytes (Fig 6a). Compared to LL/2-tumor bearing mice, LL/2-RFP-tumor bearing mice have relatively smaller tumor size and less tumor weight than LL/2-tumor bearing mice while depletion of CD4+ T cells, CD8+ T cells, or NK cells compromise the protective effect of RFP expression, which lead to bigger tumor size and significantly more tumor weight in mice (Fig. 6b-c). This means that CD4+ T cells, CD8+ T cells, and NK cells all play a role in inhibiting LL/2-RFP tumor growth *in vivo*.

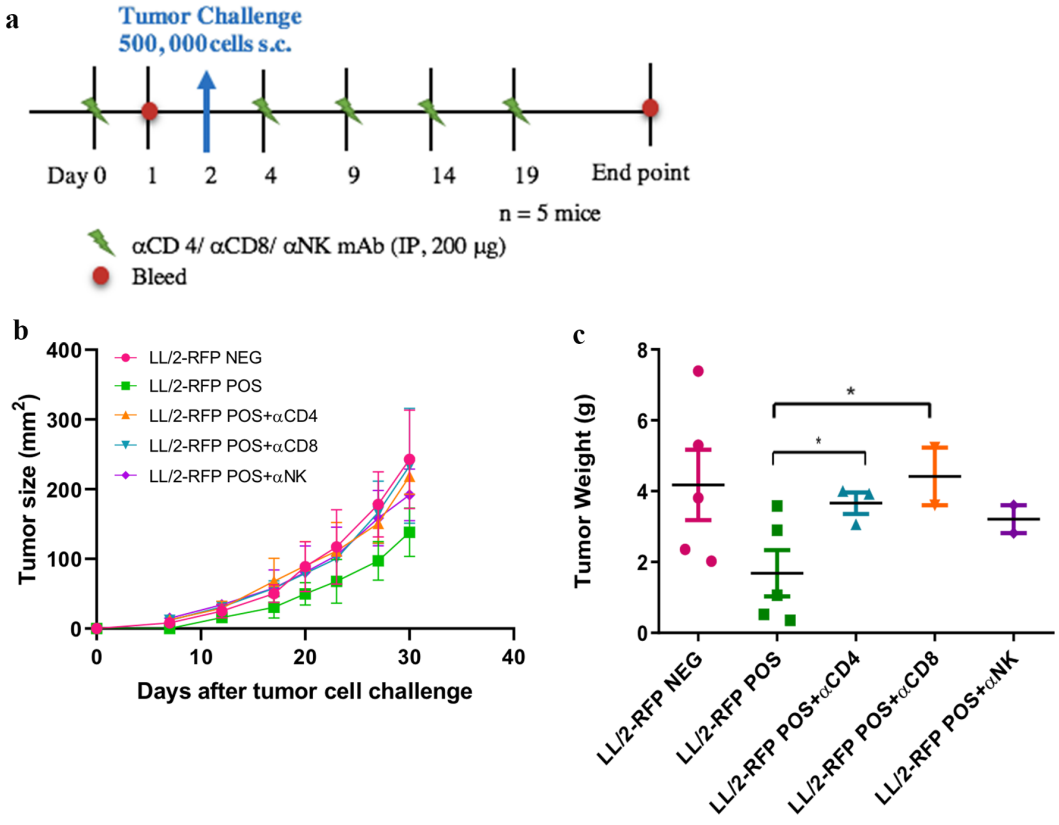

Figure 6. LL/2-RFP tumor growth is inhibited by CD4+ T cells, CD8+ T cells, NK cells *in vivo*. (a) Experimental design of *in vivo* cell depletion study. C57BL/6 mice were depleted of CD4+ T cells, CD8+ T cells, or NK cells by i.p. injection of cellular depletion antibodies (200μg/ dose). Blood samples were collected within 24 hours of the first dose of cellular depletion antibodies to confirm the efficacy of depletion. After confirmation, mice were challenged with 5×10^5 cells s.c. in the flank and subsequently injected with another four doses of cellular depletion antibodies every five days. (b) Tumor growth and (c) tumor weight of mice with different depletion treatments are shown.

Prophylactic TMV immunotherapy induces immune cell infiltration in the LL/2 tumors but does not protect mice from tumor challenge

Next, to investigate whether transfection of RFP induce a more robust anti-tumor immunity in response to TMV immunotherapy in LL/2-RFP-tumor bearing mice, we conducted a prophylactic vaccination study. C57BL/6 mice were given 2 doses of TMVs (200μg) on Day 0 and 14 into one flank and were challenged with 5 x 10^5 tumor cells s.c. in the opposite flank. At

the IACUC end point, tumor tissue and blood samples from the facial vein were collected (Fig. 7a). We observed that mice immunized with TMV immunotherapy had indistinguishable tumor weight and lung metastasis cell counts compared to the PBS control (Fig. 7b-c). However, flow cytometry analysis of TILs indicates that there were significantly more CD4+ T cells, CD8+ T cells, and B cells infiltration in vaccinated group than unvaccinated group (Fig. 7d-f). These data demonstrate that although TMV immunotherapy induces immune cell infiltration in the LL/2 tumors, it still does not protect mice from LL/2 tumor cell challenge.

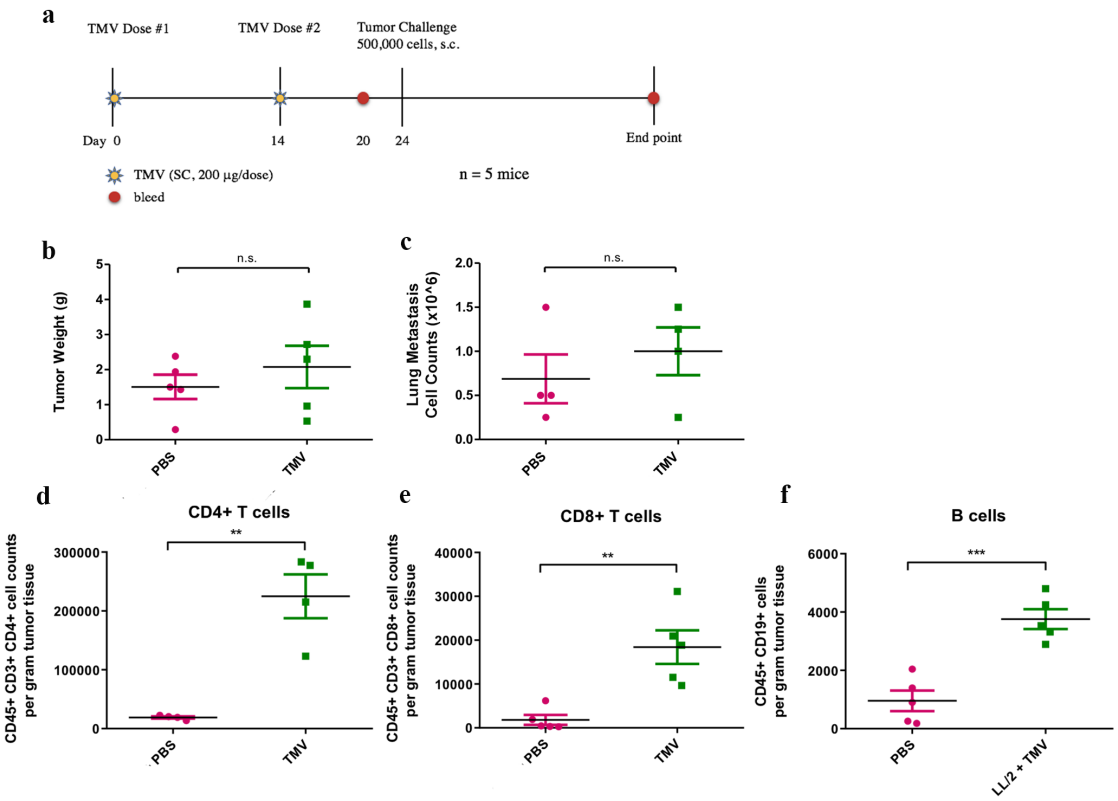

Figure 7. TMV immunotherapy induces immune cell infiltration in the LL/2 tumors but does not protect mice from tumor cell challenge. (a) Experimental design of prophylactic vaccination study. C57BL/6 mice (n=5) were given 2 doses of TMVs (200µg) on Day 0 and 14 into one flank and were challenged with 5 x 10^5 tumor cells s.c. in the opposite flank. At the IACUC end point, tumor tissue and blood samples from the facial vein were collected. (b) Tumor weight measured at the IACUC end point of mice with or without TMV immunotherapy. (c) Lungs were collected from the mice and prepared single cell suspension. Then the cells were treated with G418 (400ng/ml) in 6-well plates for 3 days to remove fibroblasts and then cultured in fresh media to detect lung metastasis. Cells were counted when one of the wells reached confluency. (d-f) CD4+

T cells, CD8+ T cells, and B cells infiltration in TMV-vaccinated and control group in LL/2 tumor model were analyzed by flow cytometry.

Prophylactic TMV vaccination inhibits primary and metastatic tumor growth and induces tumor immunogenicity in the mice challenged with LL/2-RFP tumor cells

Compared to LL/2-tumor bearing mice, mice challenged with LL/2-RFP cells benefited from TMV immunotherapy, as indicated by significantly reduced primary tumor weight and metastatic lung cells in the TMV-vaccinated mice challenged with LL/2-RFP cells (Fig. 8a-b). As previous data has shown, RFP transfection of LL/2 cells induces significantly more CD4+ T cells, CD8+ T cells, and B cells in tumor tissue (Fig. 8e-g). TMV immunotherapy induces even more CD4+ T cell and CD8+ T cell infiltration in LL/2-RFP tumors compared to the PBS control (Fig. 8e-g).

Next, to investigate whether the immunosuppressive MDSCs and MDSC-inducing factor, G-CSF are downregulated in TMV-mediated protection, a flow cytometry analysis was performed to check the level of MDSC in blood and G-CSF ELISA was conducted to quantify its secretion in blood. As we expected, prophylactic TMV immunotherapy significantly decreased MDSC and G-CSF secretion in the LL/2-RFP tumor bearing mice compared to the PBS control (Fig. 8c-d). Hence, this study demonstrates that RFP transfection of LL/2 cells induces anti-tumor immunity by inhibiting tumor induced G-CSF and MDSC levels in response to TMV immunotherapy, which leads to inhibition of primary and metastatic tumor growth.

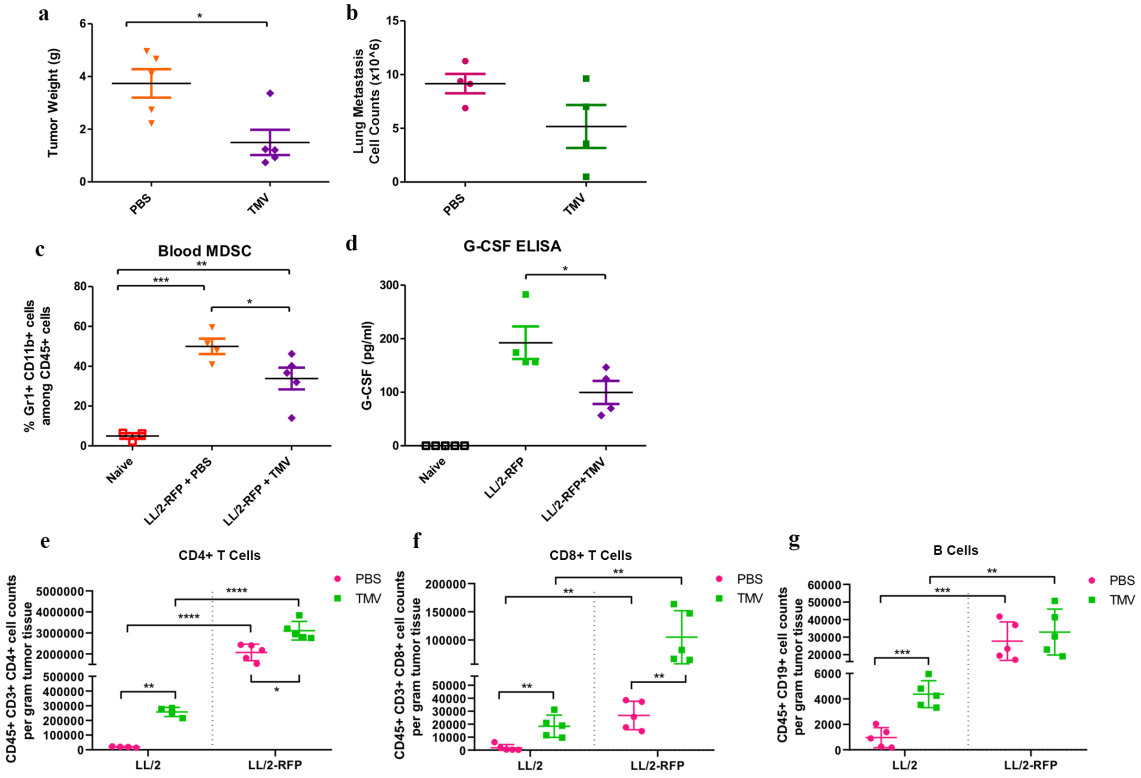

Figure 8. TMV vaccination inhibits primary and metastatic tumor growth and induces tumor immunogenicity in the mice challenged with LL/2-RFP tumor cells. (a-b) TMV immunotherapy inhibits primary and metastatic tumor growth in the mice challenged with LL/2-RFP cells. (c) TMV immunotherapy decreases MDSC and (d) G-CSF secretion in plasma of the LL/2-RFP tumor bearing mice. (e-f) CD4+ T cells, CD8+ T cells, and B cells infiltration in TMV-vaccinated and control group in LL/2-RFP tumor model was analyzed by flow cytometry.

PROJECT II

DISCUSSION

Our studies demonstrate that transfection of LL/2 cell line with a foreign antigen, red fluorescent protein does not change its morphologic features, but converts it to an immunogenic tumor model. This is supported by observations that LL/2 tumors are highly tumorigenic and ICI therapy or the combination of ICI therapy with other immunotherapies, including TMV cannot induce anti-tumor immune response in mice. However, the expression of RFP in LL/2 cells induces tumor immunogenicity by inducing TILs and inhibiting tumor induced G-CSF and MDSC levels. In addition, prophylactic TMV immunotherapy prime the immune system and boost the anti-tumor immune response in LL/2-RFP-tumor bearing mice by further inducing TILs and inhibiting tumor induced G-CSF and MDSC levels.

Our data show that LL/2-tumor bearing mice have a higher level of G-CSF and MDSC in blood, a lower level of TILs, and bigger tumor size. We hypothesize that LL/2 tumor cells induce secretion of G-CSF by fibroblasts and/ or immune cells in the tumor microenvironment, which induces MDSC production. MDSC then infiltrate to the tumor site and inhibit T lymphocytes. As a result, LL/2 tumor cells proliferate, and the cycle continues (Fig. 9a). On the other hand, LL/2-RFP-tumor bearing mice have a lower level of G-CSF and MDSC in blood, a higher level of TILs, and smaller tumor size. The possible mechanism in RFP-mediated anti-tumor effect is that the RFP foreign antigen presentation on tumor cells prime and activate immune cells, which induces more infiltration of T lymphocytes in tumor tissue. T lymphocytes then kill the tumor cells and less G-CSF secretion is induced, and thus results in less MDSC. Hence, MDSC inhibition of T cells is blocked (Fig. 9b).

However, although RFP expression can induce some anti-tumor immunity, mice cannot get complete protection against tumor growth. Therefore, we investigate whether prophylactic TMV immunotherapy induces a more robust anti-tumor immune response in LL/2-RFP-tumor

bearing mice. In TMV-vaccinated mice with LL/2 cell challenge, they have bigger tumors and a higher level of G-CSF and MDSC. Interestingly, they also have a higher level of TILs. Our hypothesis is that two counteracting mechanisms occur in these mice. Although TMVs present tumor antigens to prime and activate immune cells in mice to infiltrate into the tumor tissue, this effect is compromised by the malignancy and tumorigenicity of LL/2 tumor cells, which rapidly induce the production of immunosuppressive MDSC by G-CSF secretion (Fig. 9c). Finally, in the TMV-vaccinated mice with LL/2-RFP tumor cell challenge, they have smaller tumors, a higher level of TILs, and a lower level of G-CSF and MDSC. In these mice, both RFP expression and TMV present foreign antigens to prime and activate immune cells, which double the effect, leading to a much higher level of TILs. TILs kill the tumor cells and results in less G-CSF secretion, and thus less MDSC production (Fig. 9d).

Furthermore, our previous studies show that LL/2 tumor model is fully ICI-resistant. Since both LL/2 and LL/2-RFP cells express PD-L1, further studies are required to investigate whether the expression of RFP induces anti-tumor immunity in response to ICI therapy, such as anti-PD-1 and anti-CTLA-4 antibodies, or in combination with TMV immunotherapy. Also, more studies are needed to determine whether the ISM-incorporated TMV vaccine can induce a complete protection against primary tumor growth and/ or metastatic tumor burden in LL/2-RFP tumor model. In summary, these studies show that transfection of a murine cancer model with a foreign antigen is possible to induce tumor immunogenicity by increasing TILs while inhibiting immunosuppressive MDSC levels in response to TMV immunotherapy.

a

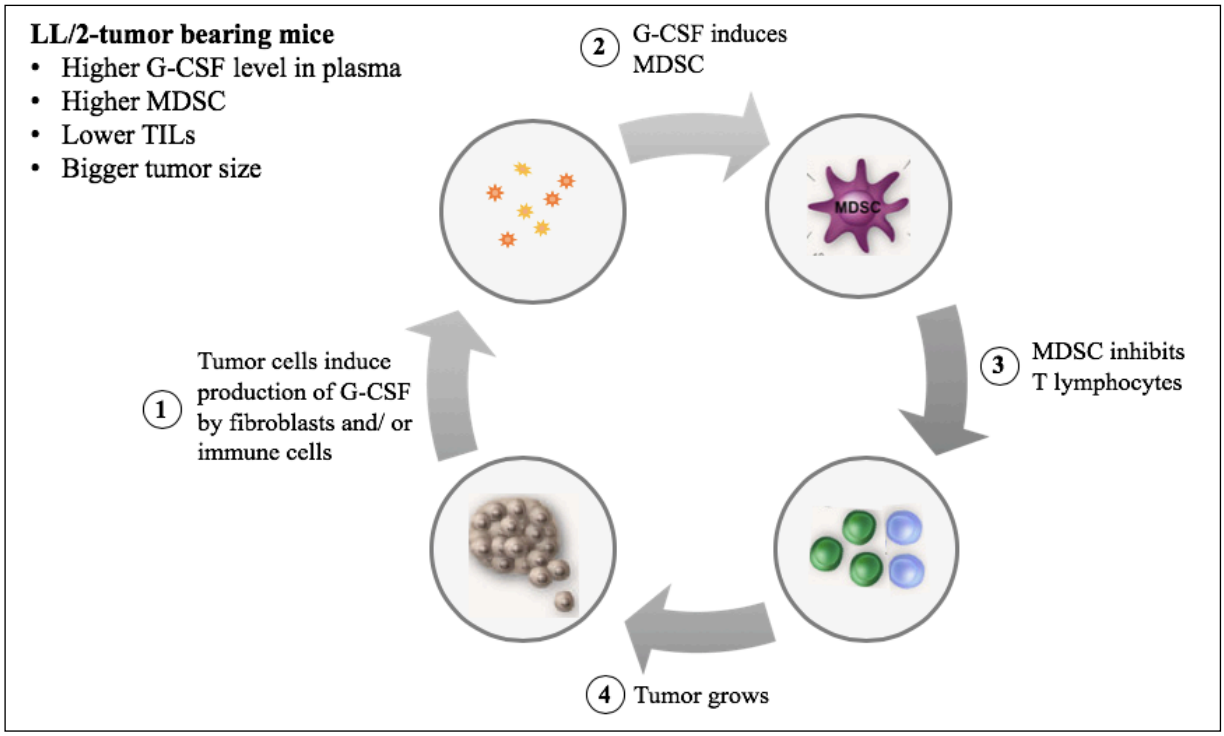
LL/2-tumor bearing mice
• Higher G-CSF level in plasma
• Higher MDSC
• Lower TILs
• Bigger tumor size
2 G-CSF induces MDSC
MDSC
3 MDSC inhibits T lymphocytes
4 Tumor grows
1 Tumor cells induce production of G-CSF by fibroblasts and/ or immune cells

b

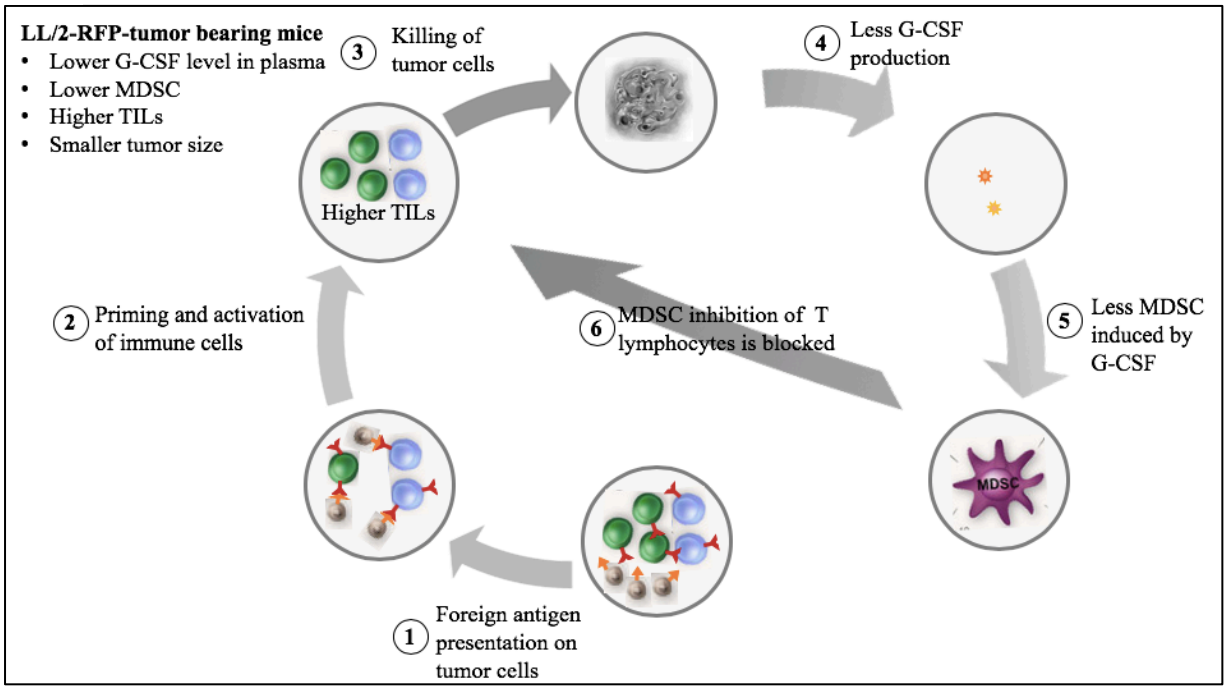
LL/2-RFP-tumor bearing mice
• Lower G-CSF level in plasma
• Lower MDSC
• Higher TILs
• Smaller tumor size
3 Killing of tumor cells
4 Less G-CSF production
Higher TILs
2 Priming and activation of immune cells
6 MDSC inhibition of T lymphocytes is blocked
5 Less MDSC induced by G-CSF
MDSC
1 Foreign antigen presentation on tumor cells

c

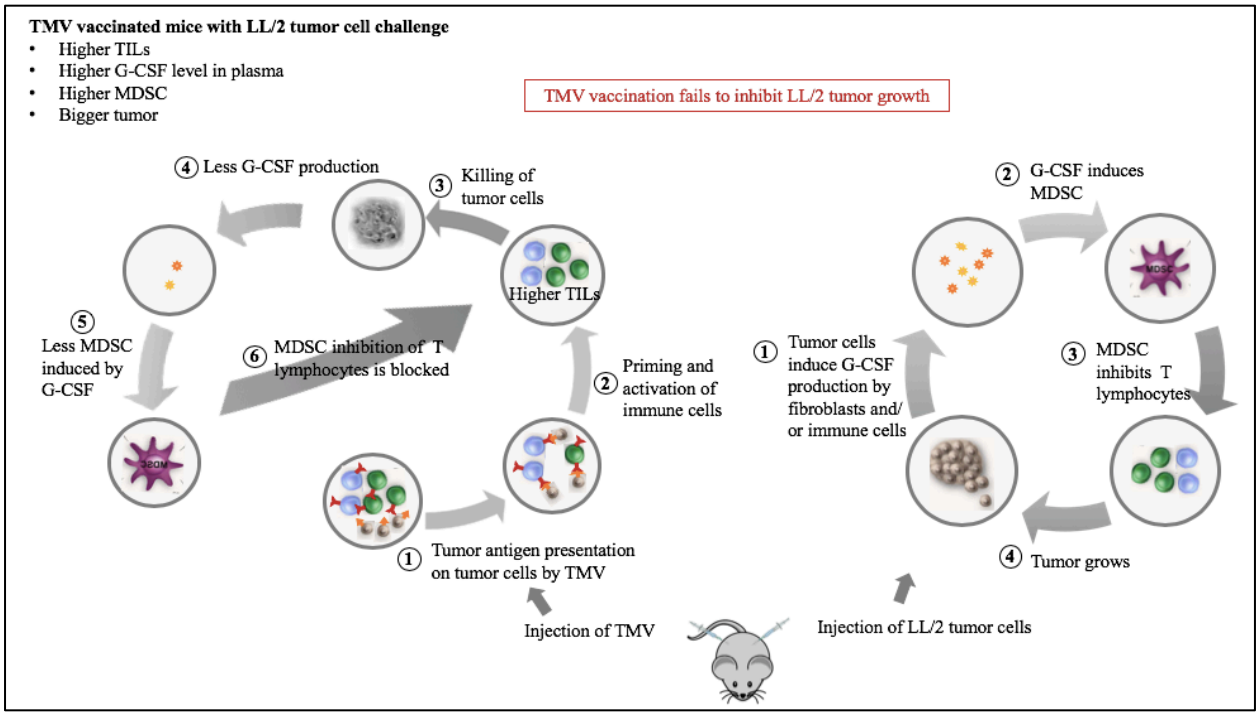

d

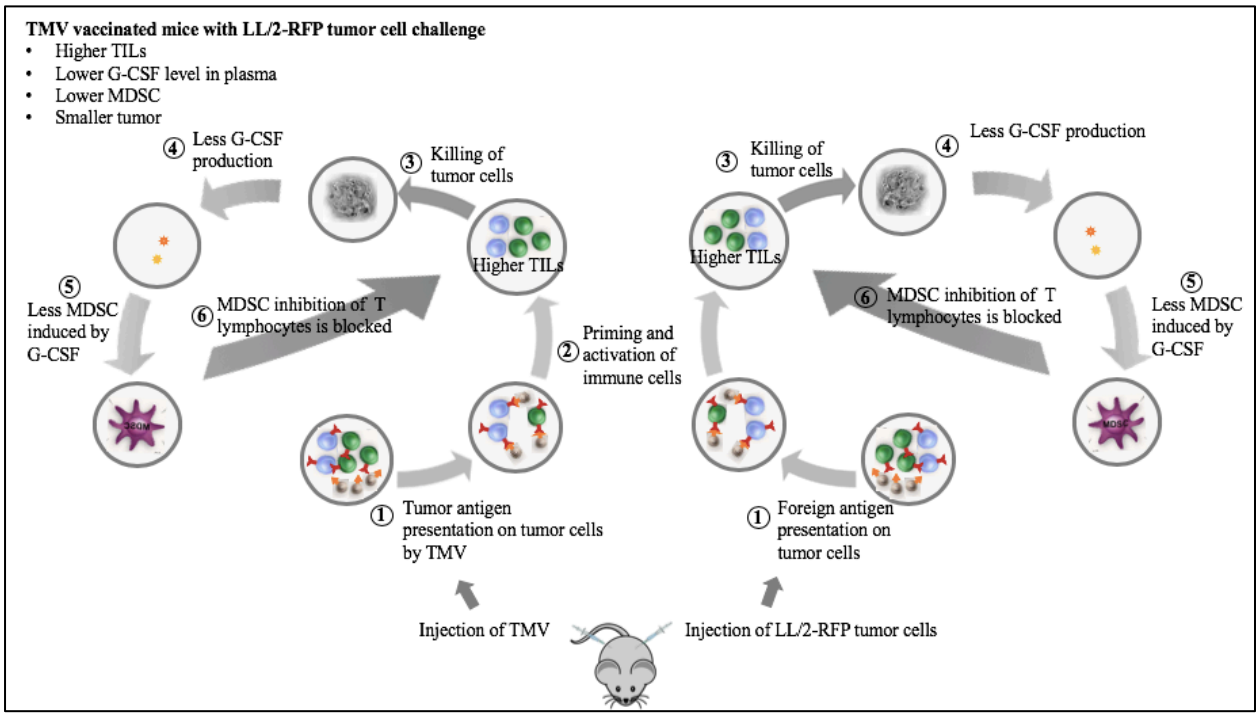

Figure 9. Schematic representations of RFP and TMV-mediated anti-tumor immune response in LL/2 tumor model. (a-b) Schematic representation of RFP-mediated anti-tumor immune response in LL/2 and LL/2-RFP-tumor bearing mice. (c-d) Schematic representation of TMV vaccinated mice challenged with LL/2 or LL/2-RFP tumor cells.

REFERENCES

1. Dela Cruz, C.S., Tanoue, L.T. & Matthay, R.A. Lung cancer: epidemiology, etiology, and prevention. *Clin Chest Med* **32**, 605-644 (2011).

2. Siegel, R.L., Miller, K.D. & Jemal, A. Cancer statistics, 2019. *CA Cancer J Clin* **69**, 7-34 (2019).

3. Esposito, L., Conti, D., Ailavajhala, R., Khalil, N. & Giordano, A. Lung Cancer: Are we up to the Challenge? *Curr Genomics* **11**, 513-518 (2010).

4. Gadgeel, S.M., Ramalingam, S.S. & Kalemkerian, G.P. Treatment of lung cancer. *Radiol Clin North Am* **50**, 961-974 (2012).

5. Grigg, C. & Rizvi, N.A. PD-L1 biomarker testing for non-small cell lung cancer: truth or fiction? *J Immunother Cancer* **4**, 48 (2016).

6. Nagarajan, S. & Selvaraj, P. Glycolipid-anchored IL-12 expressed on tumor cell surface induces antitumor immune response. *Cancer Res* **62**, 2869-2874 (2002).

7. Leonard, J.P. *et al.* Effects of single-dose interleukin-12 exposure on interleukin-12-associated toxicity and interferon-gamma production. *Blood* **90**, 2541-2548 (1997).

8. Chen, L. & Flies, D.B. Molecular mechanisms of T cell co-stimulation and co-inhibition. *Nat Rev Immunol* **13**, 227-242 (2013).

9. Trinchieri, G. & Scott, P. Interleukin-12: basic principles and clinical applications. *Curr Top Microbiol Immunol* **238**, 57-78 (1999).

10. Franks, L.M., Carbonell, A.W., Hemmings, V.J. & Riddle, P.N. Metastasizing tumors from serum-supplemented and serum-free cell lines from a C57BL mouse lung tumor. *Cancer Res* **36**, 1049-1055 (1976).

11. Hung, K. *et al.* The central role of CD4(+) T cells in the antitumor immune response. *J Exp Med* **188**, 2357-2368 (1998).

12. Farkona, S., Diamandis, E.P. & Blasutig, I.M. Cancer immunotherapy: the beginning of the end of cancer? *BMC Med* **14**, 73 (2016).

13. Jin, H.T., Ahmed, R. & Okazaki, T. Role of PD-1 in regulating T-cell immunity. *Curr Top Microbiol Immunol* **350**, 17-37 (2011).

14. Bertram, J.S. & Janik, P. Establishment of a cloned line of Lewis Lung Carcinoma cells adapted to cell culture. *Cancer Lett* **11**, 63-73 (1980).

15. Chesney, J.A., Mitchell, R.A. & Yaddanapudi, K. Myeloid-derived suppressor cells-a new therapeutic target to overcome resistance to cancer immunotherapy. *J Leukoc Biol* **102**, 727-740 (2017).

16. Pozo, A.L., Godfrey, E.M. & Bowles, K.M. Splenomegaly: investigation, diagnosis and management. *Blood Rev* **23**, 105-111 (2009).

17. Bronte, V. & Pittet, M.J. The spleen in local and systemic regulation of immunity. *Immunity* **39**, 806-818 (2013).

18. Ostrand-Rosenberg, S. & Sinha, P. Myeloid-derived suppressor cells: linking inflammation and cancer. *J Immunol* **182**, 4499-4506 (2009).

19. Umansky, V., Blattner, C., Gebhardt, C. & Utikal, J. The Role of Myeloid-Derived Suppressor Cells (MDSC) in Cancer Progression. *Vaccines (Basel)* **4** (2016).

20. Ravindranathan, S. *et al.* Tumor-derived granulocyte colony-stimulating factor diminishes efficacy of breast tumor cell vaccines. *Breast Cancer Res* **20**, 126 (2018).